

PFC/JA-84-37

KINETIC EQUILIBRIUM PROPERTIES
OF RELATIVISTIC NONNEUTRAL ELECTRON
FLOW IN A CYLINDRICAL DIODE
WITH APPLIED MAGNETIC FIELD

Han S. Uhm
Ronald C. Davidson

October, 1984

KINETIC EQUILIBRIUM PROPERTIES OF RELATIVISTIC NONNEUTRAL
ELECTRON FLOW IN A CYLINDRICAL DIODE WITH APPLIED MAGNETIC FIELD

Han S. Uhm
Naval Surface Weapons Center, Silver Spring, MD 20910

Ronald C. Davidson
Plasma Fusion Center
Massachusetts Institute of Technology, Cambridge, MA 02139

ABSTRACT

The equilibrium properties of a relativistic nonneutral electron layer confined in a magnetically insulated cylindrical diode are investigated within the framework of the steady-state ($\partial/\partial t=0$) Vlasov-Maxwell equations. The analysis is carried out for an infinitely long electron layer aligned parallel to a uniform externally applied magnetic field $B_0 \hat{e}_z$, which provides radial confinement of the electrons. The theoretical analysis is specialized to the class of self-consistent Vlasov equilibria $f_b^0(x, p)$ in which all electrons have the same canonical angular momentum ($P_\theta = P_0 = \text{const.}$), and the same energy ($H = mc^2$), i.e., $f_b^0 = (\hat{n}_b R_c / 2\pi m) \delta(H - mc^2) \delta(P_\theta - P_0)$. One of the most important features of the analysis is that the closed analytic expressions for the self-consistent electrostatic potential $\phi_0(r)$ and the θ -component of vector potential $A_0(r)$ are obtained. Moreover, all essential equilibrium quantities, such as electron density profile $n_b^0(r)$, total magnetic field $B_{0z}(r)$, perpendicular temperature profile $T_{\perp b}^0(r)$, etc., can be calculated self-consistently from these potentials. As a special case, the equilibrium properties of a planar diode are investigated in the limit of large aspect ratio, further simplifying the functional form of the electrostatic and vector potentials. Detailed equilibrium properties are investigated numerically for a cylindrical diode over a broad range of system parameters, including diode voltage V_0 , cathode electric field, electron density \hat{n}_b at the cathode, diode polarity, and externally applied magnetic field B_0 .

I. INTRODUCTION AND SUMMARY

There is a growing literature¹⁻⁷ on theoretical studies of the equilibrium and stability properties of sheared, nonneutral electron flow in cylindrical and planar models of high-voltage diodes with application to the generation of intense charged particle beams for inertial confinement fusion.^{8,9} These analyses¹⁻⁷ have represented major extensions of earlier work¹⁰⁻¹⁷ to include the important influence of cylindrical,¹ relativistic,²⁻⁵ electromagnetic,²⁻⁵ nonlinear,⁶ and kinetic⁷ effects on equilibrium and stability properties at moderately high electron density. While an understanding of the important physics issues is increasing, the majority¹⁻⁶ of these studies have been based on macroscopic cold-fluid models, largely for reasons of analytical and numerical convenience. In the present article, we make use of the steady-state ($\partial/\partial t = 0$) Vlasov-Maxwell equations to investigate the equilibrium properties of sheared, relativistic, nonneutral electron flow in a cylindrical diode. The analysis is based on well-established theoretical techniques^{16,18-21} developed in basic studies of the kinetic equilibrium and stability properties of nonneutral electron plasmas characterized by intense self fields. Since the present treatment is fully kinetic, the effects of finite temperature and large orbit excursions are included in a fully self-consistent manner. As a general remark, in circumstances involving the generation of intense ion beams, unstable field perturbations may cause large ion deflections, and poor beam collimation. Therefore, any modification of equilibrium and stability properties associated with electron kinetic effects (e.g., finite temperature, etc.) may be of considerable importance in determining the conditions for optimum diode performance.

To briefly summarize, the equilibrium properties of a relativistic nonneutral electron layer confined in a magnetically insulated cylindrical diode are investigated within the framework of the steady-state ($\partial/\partial t = 0$) Vlasov-Maxwell equations. The theoretical model and assumptions are described in Sec. II, and the detailed analytical investigations and numerical results are presented in Secs. III and IV, and in Sec. V, respectively. The analysis is carried out for an infinitely long electron layer aligned parallel to a uniform, externally applied magnetic field $B_0 \hat{e}_z$, which provides radial confinement of the electrons (Fig. 1). Moreover, we specialize to the class of self-consistent Vlasov equilibria $f_b^0(x, p)$ in which all electrons have the same canonical angular momentum ($P_\theta = P_0 = \text{const.}$) and the same energy ($H = mc^2$).¹⁸⁻²¹ That is, $f_b^0(x, p)$ is specified by [Eq. (15)]

$$f_b^0 = \frac{\hat{n}_b R_c}{2\pi m} \delta(H - mc^2) \delta(P_\theta - P_0),$$

where $H = (m^2 c^4 + c^2 p_\perp^2)^{1/2} - e\phi_0(r)$ is the energy, and $P_\theta = r[p_\theta - eA_0(r)/c]$ is the canonical angular momentum. One of the most important features of the analysis in Secs. II-IV is that closed analytic expressions are obtained for the self-consistent electrostatic potential $\phi_0(r)$ and the θ -component of vector potential $A_0(r)$. Moreover, all essential equilibrium quantities, such as electron density profile $n_b^0(r)$, total magnetic field $B_{0z}(r)$, perpendicular temperature profile $T_{\perp b}^0(r)$, etc., are calculated self-consistently from these potentials. As a special case, the equilibrium properties of a planar diode are investigated in Sec. IV in the limit of large aspect ratio, further simplifying the functional form of the electrostatic and vector potentials. It is shown analytically that the transverse temperature of the electron layer

in the planar case vanishes identically for space-charge-limited flow with zero electric field at the cathode.

Although both diode polarities are investigated in Secs. II-V, we limit the present summary in Sec. I to the case of positive diode polarity ($p=+1$). That is, in Fig. 1, the cathode is located at the inner conductor ($R_c = a$) with $\phi_0(r=a) = 0$, and the anode is located at the outer conductor with $\phi_0(r=b) = V_0$, where V_0 is the applied voltage. Moreover, in the expression for $f_b^0(x, p)$ in Eq. (15), \hat{n}_b is the density at the cathode, and the constant P_0 is defined by $P_0 = -(ea/c)A_0(a)$ [Eq. (16)], corresponding to zero average azimuthal flow of electrons at the cathode ($r=a$). We also introduce the definitions [Eqs. (18) and (20)]

$$\gamma(r) = 1 + \frac{e\phi_0(r)}{mc^2} ,$$

$$\delta A_0(r) = A_0(r) - \frac{a}{r} A_0(r=a) ,$$

where $\phi_0(r)$ is the electrostatic potential, and $A_0(r)$ is the vector-potential for the total (applied plus self) magnetic field. Some straightforward algebra shows that the density profile $n_b^0(r) = \int d^3p f_b^0$ corresponding to Eq. (15) is given by [Eq. (24)]

$$n_b^0(r) = \begin{cases} \frac{\gamma(r)\hat{n}_b a}{r} , & p_{\perp 0}^2(r) \geq 0 , \\ 0 , & \text{otherwise} , \end{cases}$$

where $p_{\perp 0}^2(r)$ is defined by [Eq. (22)]

$$p_{\perp 0}^2(r) = [\gamma^2(r) - 1]m^2c^2 - \left[\frac{e}{c} \delta A_0(r)\right]^2 .$$

The outer boundary of the electron layer (denote by $r = \hat{R}_b$) is determined self-consistently from $p_{\perp 0}^2(\hat{R}_b) = 0$. It is also found that the azimuthal

flux of electrons $n_b^0 v_{\theta b}^0(r) = \int d^3 p v_{\theta b} f_b^0$ is given by [Eq. (26)]

$$n_b^0(r) v_{\theta b}^0(r) = \frac{a}{r} \frac{\hat{n}_b e}{mc} \delta A_0(r)$$

for $a \leq r \leq R_b$. Moreover, the effective perpendicular ($r-z$) temperature

$T_{\perp b}^0(r)$ defined by $n_b^0 T_{\perp b}^0 = (1/2) \int d^3 p c^2 (p_r^2 + p_z^2) f_b^0 / (m^2 c^4 + c^2 p_{\perp}^2)^{1/2}$, is given by [Eq. (27)]

$$T_{\perp b}^0(r) = \frac{p_{\perp 0}^2(r)}{2\gamma(r)m}$$

for $a \leq r \leq R_b$. What is most remarkable, is that the Maxwell equations for $\phi_0(r)$ and $\delta A_0(r)$ permit exact analytic solutions for the equilibrium potentials for the choice of distribution function in Eq. (15) and general aspect ratio of the diode. For example, introducing the normalized radial variable $\xi = (2\hat{\omega}_{pb}/c)(ra)^{1/2}$, where $\hat{\omega}_{pb}^2 = 4\pi\hat{n}_b e^2/m$, the exact solution to the equilibrium Poisson equation (28) is [Eq. (42)]

$$\begin{aligned} \gamma(r) = 1 + \frac{e\phi_0(r)}{mc^2} &= \rho [K_1(\rho) I_0(\xi) + I_1(\rho) K_0(\xi)] \\ &+ 2\alpha [K_0(\rho) I_0(\xi) - I_0(\rho) K_0(\xi)] \end{aligned}$$

for $a \leq r \leq R_b$. Here $\rho = 2\hat{\omega}_{pb} a/c$, and I_n and K_n are modified Bessel functions of order n . Moreover, the dimensionless parameter α is a measure of the electric field (apart from a sign) at the cathode and is defined by [Eq. (32)]

$$\alpha = \frac{ea}{mc^2} \left(\frac{\partial \phi_0}{\partial r} \right)_{r=a}$$

In the vacuum region ($R_b \leq r \leq b$) outside the electron layer, the solution for $\gamma(r) = 1 + e\phi_0/mc^2$ that is continuous with continuous first derivative at $r=R_b$ is given by [Eq. (53)]

$$\gamma(r) = \gamma(R_b) + \alpha_b \ln(r/R_b),$$

where $\gamma(R_b)$ and $\alpha_b \equiv R_b (\partial\gamma/\partial r)_{r=R_b}$ are evaluated from Eq. (42). Moreover, enforcing $\phi_0(r=b) = V_0$, where V_0 is the applied voltage gives [Eq. (54)]

$$\frac{eV_0}{mc^2} = [\gamma(R_b) - 1] + \alpha_b \ln(b/R_b),$$

which relates the diode voltage to the other equilibrium parameters.

In a similar manner, the θ -component of vector potential $A_0(r)$ can be evaluated in closed analytic form [Eq. (48)], and the total (applied plus self) magnetic field determined from $B_{0z}(r) = (1/r)(\partial/\partial r)(rA_0)$. Denoting the vacuum value of $B_{0z}(r)$ by $B_0 = \text{const.}$ in the region $R_b \leq r \leq b$, it is found for a diode with positive polarity ($p=+1$) that $B_{0z}(r)$ decreases monotonically from B_0 at the boundary of the electron layer ($r=R_b$) to the value $B_{0z}(a) < B_0$ at the cathode ($r=a$) where [Eq. (55)]

$$\frac{B_{0z}(a)}{B_0} = \frac{R_b/a\eta}{K_2(\rho)I_1(\eta) + I_2(\rho)K_1(\eta)}.$$

Here, $\rho \equiv 2\hat{\omega}_{pb}a/c$ and $\eta \equiv (R_b/a)^{1/2}\rho$.

Finally, in Sec. V, the detailed equilibrium properties of a cylindrical diode are investigated numerically over a broad range of system parameters, including diode voltage V_0 , diode polarity ($p=\pm 1$), cathode electric field (α), electron density \hat{n}_b at the cathode, applied magnetic field B_0 , and the ratio b/a of the inner and outer conductor radii. Several features are noteworthy in this analysis. First, the electron layer in a positive polarity diode ($p=+1$) exhibits diamagnetic behavior, whereas the electron layer in a negative polarity diode ($p=-1$) exhibits

paramagnetic properties. Indeed, a negative polarity diode is more effective in confining the electrons because the magnetic field in the anode region is larger than the externally applied magnetic field B_0 . Second, the layer thickness decreases with increasing applied magnetic field B_0 . However, the layer thickness is an increasing function of diode voltage V_0 . Third, the density of the electron layer increases with applied magnetic field B_0 . Fourth, the transverse temperature $T_{\perp b}^0(r)$ increases substantially as the strength of the electric field at the cathode is increased. We therefore find that the density of the electron layer decreases as the electric field at the cathode is increased.

II. THEORETICAL MODEL AND BASIC ASSUMPTIONS

The equilibrium configuration is illustrated in Fig. 1. It consists of a nonneutral, pure electron plasma that is infinite in axial extent and aligned parallel to a uniform applied magnetic field $\mathbf{B}_0^{\text{ext}} = B_0 \hat{e}_z$, where \hat{e}_z is a unit vector in the z-direction. The applied axial magnetic field provides radial confinement of the electrons between the cathode and radius R_b . The radii of the inner and outer conductors are denoted by a and b , respectively. As shown in Fig. 1, we introduce a cylindrical polar coordinate system (r, θ, z) with z-axis coinciding with the axis of symmetry; r is the radial distance from the z-axis; and θ is the polar angle in a plane perpendicular to the z-axis. The region of configuration space described in the present analysis is limited to the region between the inner and outer conductors, i.e., $a \leq r \leq b$. The electrons are emitted from the cathode at radius $r=R_c$ and are accelerated towards the anode by the radial electric field. The $\mathbf{v} \times \mathbf{B}_0$ force produced by the axial magnetic field converts radial electron motion into azimuthal motion, and eventually the electrons reverse their radial velocity and return to the cathode. The mean azimuthal flow of the electrons produces an axial self magnetic field as shown in Fig. 1.

In the equilibrium analysis, we allow both electric field polarities. Positive polarity is defined by

$$p = +1, \quad (1)$$

where the potential of the cathode at the inner conductor is

$\phi_0(r=a)=0$, and the potential of the anode at the outer conductor is

$\phi_0(r=b)=V_0$. On the other hand, negative polarity is defined by

$$p = -1 , \quad (2)$$

where the cathode is located at the outer conductor with $\phi_0(r=b) = 0$, and the anode is located at the inner conductor with $\phi_0(r=a) = V_0$. Therefore, for the two polarities, the cathode radius R_c is given by

$$R_c = \begin{cases} a , & p=+1 , \\ b , & p=-1 . \end{cases} \quad (3)$$

To make the theoretical analysis tractable, the following simplifying assumptions are made in describing the nonneutral plasma equilibrium by the steady-state ($\partial/\partial t=0$) Vlasov-Maxwell equations:

(a) Equilibrium properties are independent of z ($\partial/\partial z=0$) and azimuthally symmetric ($\partial/\partial \theta=0$) about the z -axis. For example, the electrostatic potential $\phi_0(\mathbf{x}) = \phi_0(r)$ is a function only of the radial coordinate r .

(b) Although an individual electron can move in the radial and axial directions, there is no mean motion of the electrons in these directions, i.e.,

$$\int d^3p \, v_r \, f_b^0(\mathbf{x}, \mathbf{p}) = 0 = \int d^3p \, v_z \, f_b^0(\mathbf{x}, \mathbf{p}) .$$

Since the axial current is equal to zero, there is no self magnetic field in the θ -direction.

(c) The kinetic energy of the electrons at the cathode ($r=R_c$) is equal to zero. This also implies that there is no azimuthal motion of the electrons at the cathode.

Central to a Vlasov description of nonneutral plasma equilibria are the single-particle constants of the motion in the equilibrium

field configuration.¹⁸ Within the context of Assumptions (a) and (b), the external and self magnetic fields can be expressed as

$$\vec{B}_0^{\text{ext}}(\vec{x}) = B_0 \hat{e}_z = \frac{1}{r} \frac{\partial}{\partial r} [r A_0^{\text{ext}}(r)] \hat{e}_z ,$$

and

$$\vec{B}_0^{\text{s}}(\vec{x}) = B_0^{\text{s}}(r) \hat{e}_z = \frac{1}{r} \frac{\partial}{\partial r} [r A_0^{\text{s}}(r)] \hat{e}_z ,$$

where $A_0^{\text{ext}}(r) = r B_0 / 2$, and $A_0^{\text{s}}(r)$ is the θ -component of the vector potential for the axial self magnetic field. In addition, the external and self electric fields can be expressed as

$$\begin{aligned} \vec{E}_0(\vec{x}) &= (E_{0r}^{\text{ext}} + E_{0r}^{\text{s}}) \hat{e}_r \\ &= E_{0r}(r) \hat{e}_r = - \frac{\partial}{\partial r} \phi_0(r) \hat{e}_r , \end{aligned}$$

where \hat{e}_r is a unit vector in the radial direction. For azimuthally symmetric equilibria with $\partial/\partial\theta=0$ and $\partial/\partial z=0$, there are three single-particle constants of the motion. These are the total energy H ,

$$H = (m^2 c^4 + c^2 p_\perp^2)^{1/2} - e \phi_0(r) , \quad (4)$$

the canonical angular momentum P_θ ,

$$P_\theta = r[p_\theta - (e/c)A_0(r)] , \quad (5)$$

and the axial canonical momentum P_z ,

$$P_z = p_z . \quad (6)$$

Here, c is the speed of light in vacuo, and $-e$ and m are the electron charge and rest mass, respectively. In Eqs. (4) - (6), lower case p denotes mechanical momentum, which is related to the particle velocity v by

$$v = p [m(1 + p^2/m^2 c^2)^{1/2}]^{-1} . \quad (7)$$

In Eq. (5), $A_0(r)$ is the θ -component of vector potential for the total axial magnetic field, i.e.,

$$A_0(r) = \frac{1}{2} r B_0 + A_0^s(r) . \quad (8)$$

Any distribution function $f_b^0(x, p)$ that is a function only of the single-particle constants of the motion in the equilibrium fields satisfies the steady-state ($\partial/\partial t=0$) Vlasov equation. For present purposes, we consider the class of self-consistent equilibrium distribution functions that depend on the constants H and P_θ but not explicitly on the axial momentum p_z . That is, we consider distribution functions of the form¹⁸

$$f_b^0(x, p) = f_b^0(H, P_\theta) . \quad (9)$$

As shown at the end of Sec. II, the equilibrium described by Eq. (9) generally has non-zero axial and radial temperatures.

For a specific choice of $f_b^0(H, P_\theta)$, the potentials for the equilibrium fields are to be calculated self-consistently from the steady-state Maxwell equations. The equilibrium Poisson equation can be

expressed as

$$\frac{1}{r} \frac{\partial}{\partial r} r \frac{\partial}{\partial r} \phi_0(r) = 4\pi e n_b^0(r) , \quad (10)$$

where $n_b^0(r)$ is the local electron density defined by

$$n_b^0(r) = \int d^3p f_b^0(H, p_\theta) . \quad (11)$$

Furthermore, the θ -component of the $\nabla \times \mathbf{B}_0$ Maxwell equation can be expressed as

$$\frac{\partial}{\partial r} \frac{1}{r} \frac{\partial}{\partial r} [r A_0(r)] = \frac{4\pi}{c} e n_b^0(r) v_{\theta b}^0(r) , \quad (12)$$

where $v_{\theta b}^0(r)$ is the mean azimuthal velocity of an electron fluid element defined by

$$n_b^0(r) v_{\theta b}^0(r) = \int d^3p v_\theta f_b^0(H, p_\theta) . \quad (13)$$

Here, v_θ is related to p_θ by Eq. (7). As a general remark, we note that any choice of equilibrium distribution function $f_b^0(H, p_\theta)$ assures that the radial and axial flux of electrons is equal to zero, since H is an even function of p_r and p_z [see Assumption (b)].

Once the functional form of $f_b^0(H, p_\theta)$ is specified, the electron density and azimuthal flux of electrons can be determined from Eqs. (11) and (13). Other properties of the equilibrium can also be calculated. For example, since H depends on p_r and p_z through the combination $p_r^2 + p_z^2$, it is straightforward to show that $\langle v_r p_r \rangle = \langle v_z p_z \rangle$, where $\langle \psi \rangle$ denotes $(\int d^3p \psi f_b^0) / (\int d^3p f_b^0)$. Therefore, we can define an

effective "transverse temperature" $T_{\perp b}^0(r)$ for the r - z motion of the electrons by the relation

$$n_b^0(r) T_{\perp b}^0(r) = \frac{1}{2} \int d^3p \frac{c^2 (p_r^2 + p_z^2)}{(m^2 c^4 + c^2 p^2)^{1/2}} f_b^0(H, p_\theta) , \quad (14)$$

where $p_r^2 + p_z^2$ is the transverse momentum-squared, and $p^2 = p_r^2 + p_z^2 + p_\theta^2$.

III. KINETIC EQUILIBRIUM PROPERTIES FOR MONOENERGETIC ELECTRONS

There is considerable latitude in the choice of equilibrium distribution function $f_b^0(H, P_\theta)$. For present purposes, we consider the class of self-consistent Vlasov equilibria in which all electrons have the same canonical angular momentum $P_\theta = P_0 = \text{const.}$, and the same energy $H = mc^2$. In this case the equilibrium distribution function can be expressed as¹⁸⁻²¹

$$f_b^0(H, P_\theta) = \frac{R_c \hat{n}_b}{2\pi m} \delta(H - mc^2) \delta(P_\theta - P_0), \quad (15)$$

where \hat{n}_b is the electron density at the cathode ($r=R_c$), and

$$P_0 = -\frac{e}{c} R_c A_0(R_c) = \text{const.} \quad (16)$$

is the canonical angular momentum of the electrons. Without loss of generality, we assume that the equilibrium electrostatic potential is equal to zero at the cathode, i.e.,

$$\phi_0(r=R_c) = 0. \quad (17)$$

From $H = mc^2$, we find that the mechanical energy of an electron is given by

$$\begin{aligned} (m^2 c^4 + c^2 p_\theta^2 + c^2 p_\perp^2)^{1/2} &= \gamma(r) mc^2 \\ &= mc^2 + e\phi_0(r), \end{aligned} \quad (18)$$

where $p_\perp^2 = p_r^2 + p_z^2$, and $\gamma(r) = 1 + e\phi_0(r)/mc^2$.

Since the electrons move on a surface of constant canonical angular momentum with $P_\theta = P_0 = \text{constant}$, we find from Eqs. (5) and

(16) that the azimuthal mechanical momentum is related to $A_0(r)$ by

$$p_\theta = \frac{e}{c} \delta A_0(r) , \quad (19)$$

where the notation

$$\delta A_0(r) \equiv A_0(r) - \frac{R_c}{r} A_0(R_c) , \quad (20)$$

has been introduced. In Eq. (20), the θ -component of the vector potential $A_0(r)$ is defined in Eq. (8). Making use of Eq. (19) to evaluate $H-mc^2$ for $P_\theta = P_0$, we find after some straightforward algebra that $H-mc^2$ can be expressed as

$$H-mc^2 = \{ [p_{\perp}^2 - p_{\perp 0}^2(r)] c^2 + \gamma^2(r) m^2 c^4 \}^{1/2} - \gamma(r) mc^2 , \quad (21)$$

where $\gamma(r) = 1 + e\phi_0(r)/mc^2$, and the quantity $p_{\perp 0}^2(r)$ is defined by

$$p_{\perp 0}^2(r) = [\gamma^2(r) - 1] m^2 c^2 - \left(\frac{e}{c} \delta A_0(r) \right)^2 . \quad (22)$$

Thus, the δ -function factor $\delta(H-mc^2)$ appearing in Eq. (15) can be expressed as

$$\delta(H-mc^2) = 2\gamma(r)m\delta[p_{\perp}^2 - p_{\perp 0}^2(r)] . \quad (23)$$

Substituting Eqs. (15) and (23) into Eq. (11) and carrying out the required momentum integration, it is straightforward to show that the electron density $n_b^0(r)$ is equal to $\gamma(r)\hat{n}_b R_c/r$ for the range of r satisfying $p_{\perp 0}^2(r) \geq 0$, and is equal to zero, otherwise, i.e.,

$$n_b^0(r) = \begin{cases} \frac{\gamma(r) \hat{n}_b R_c}{r}, & p_{i0}^2(r) \geq 0, \\ 0, & \text{otherwise} \end{cases} \quad (24)$$

One of the boundaries of the electron layer is the cathode ($r=R_c$), where $p_{i0}^2(R_c) = 0$ is satisfied. The other boundary R_b of the electron layer can be obtained numerically from the condition

$$p_{i0}^2(R_b) = 0. \quad (25)$$

Note that the electron density at $r=R_c$ is $n_b^0(R_c) = \hat{n}_b$, where $\gamma(R_c) = 1$. For the case of positive polarity with $p=+1$, the electron layer extends from $r=R_c=a$ to $r=R_b$, whereas for $p=-1$, the electron layer occupies the region from $r=R_b$ to $r=R_c=b$.

The mean azimuthal velocity of an electron fluid element $v_{\theta b}^0(r)$ is obtained by substituting Eqs. (15) and (19) into Eq. (13) and carrying out the momentum integration. After some straightforward algebra, we obtain

$$n_b^0(r) v_{\theta b}^0(r) = \frac{R_c}{r} \hat{n}_b \frac{e}{mc} \delta A_0(r), \quad (26)$$

for $p_{i0}^2(r) \geq 0$. It is obvious from Eqs. (20) and (26) that the azimuthal velocity of an electron fluid element is in the positive θ -direction for $p=+1$, and in the negative θ -direction for $p=-1$. In a similar manner, the effective transverse temperature defined in Eq. (14) can be expressed as

$$\begin{aligned}
T_{ib}^0(r) &= \frac{p_{i0}^2(r)}{2\gamma(r)m} \\
&= \frac{1}{2} mc^2 \left[\gamma - \frac{1}{\gamma} - \frac{1}{\gamma} \left(\frac{e}{mc^2} \delta A_0 \right)^2 \right],
\end{aligned} \tag{27}$$

which vanishes at the boundaries $r=R_c$ and $r=R_b$ of the electron layer.

Making use of the definition $\gamma(r) = 1 + e\phi_0(r)/mc^2$ and Eq. (24), the Poisson equation (10) can be expressed as

$$\frac{1}{r} \frac{\partial}{\partial r} r \frac{\partial}{\partial r} \gamma(r) - \frac{\hat{\omega}_{pb}^2 R_c}{c^2 r} \gamma(r) = 0, \tag{28}$$

over the range of r (between R_c and R_b) where $p_{i0}^2(r) \geq 0$ and the electron density is non-zero. In the vacuum region between R_b and the anode, the quantity $\gamma(r) = 1 + e\phi_0(r)/mc^2$ satisfies the vacuum Poisson equation

$$\frac{1}{r} \frac{\partial}{\partial r} r \frac{\partial}{\partial r} \gamma(r) = 0. \tag{29}$$

In Eq. (28),

$$\hat{\omega}_{pb}^2 = \frac{4\pi e^2 \hat{n}_b}{m}, \tag{30}$$

is the electron plasma frequency-squared at the cathode ($r=R_c$).

An obvious boundary condition for the second-order differential equation for $\gamma(r)$ in Eq. (28) is

$$\gamma(r=R_c) = 1. \tag{31}$$

We introduce the dimensionless parameter α defined by

$$\alpha = R_c \left(\frac{d\gamma}{dr} \right)_{R_c} = \frac{eR_c}{mc^2} \left(\frac{d\phi_0}{dr} \right)_{R_c} = - \frac{eR_c}{mc^2} E_r^0(r=R_c) , \quad (32)$$

which, apart from a sign, represents the normalized electric field at the cathode. In the limit when the electron plasma is so tenuous that self electric field contributions can be neglected, the parameter α is given by

$$\alpha = \begin{cases} \frac{eV_0}{mc^2} / \ln(b/a) , & p=+1 , \\ \frac{eV_0}{mc^2} / \ln(a/b) , & p=-1 , \end{cases}$$

where $p=\pm 1$ is the polarity of the diode, and V_0 is the diode voltage.

On the other hand, for space-charge-limited flow, $E_r^0(r=R_c) = 0$, and the parameter α is given by

$$\alpha = 0 .$$

Therefore, the normalized electric field α must satisfy

$$\begin{aligned} 0 \leq \alpha &< \frac{eV_0}{mc^2} / \ln(b/a) , & \text{for } p=+1 , \\ 0 \geq \alpha &> \frac{eV_0}{mc^2} / \ln(a/b) , & \text{for } p=-1 . \end{aligned} \quad (33)$$

The boundary conditions satisfied by $\gamma(r) = 1 + e\phi_0(r)/mc^2$ at the surface of the electron layer ($r=R_b$) are prescribed by the continuity of $\gamma(r)$ and its first derivative $d\gamma(r)/dr$ at $r=R_b$. That is,

$$\lim_{\delta \rightarrow 0_+} [\gamma(R_b + \delta) - \gamma(R_b - \delta)] = 0 ,$$

$$\lim_{\delta \rightarrow 0_+} \left[\left(\frac{d\gamma}{dr} \right)_{R_b + \delta} - \left(\frac{d\gamma}{dr} \right)_{R_b - \delta} \right] = 0 .$$
(34)

The differential equation for the θ -component of vector potential is obtained by substituting Eq. (26) into Eq. (12). This gives

$$\frac{d}{dr} \frac{1}{r} \frac{d}{dr} [r \delta A_0(r)] - \frac{\hat{\omega}^2 R_c}{r c^2} \delta A_0(r) = 0 ,$$
(35)

in the region between $r=R_c$ and $r=R_b$ where $p_{10}^2(r) \geq 0$ and the electron density is non-zero. In the vacuum region, δA_0 satisfies

$$\frac{d}{dr} \frac{1}{r} \frac{d}{dr} [r \delta A_0(r)] = 0 .$$
(36)

One boundary condition satisfied by Eq. (35) is

$$\delta A_0(r=R_c) = 0 .$$
(37)

Another boundary condition is

$$B_0 = \begin{cases} \frac{1}{R_b} \left\{ \frac{d}{dr} [r \delta A_0(r)] \right\}_{r=R_b} , & \text{for } p=+1 , \\ \frac{1}{b} \left\{ \frac{d}{dr} [r \delta A_0(r)] \right\}_{r=b} , & \text{for } p=-1 , \end{cases}$$
(38)

where B_0 is the externally applied vacuum magnetic field. Moreover, at the surface ($r=R_b$) of the electron layer, $\delta A_0(r)$ satisfies

$$\lim_{\delta \rightarrow 0^+} [\delta A_0(R_b + \delta) - \delta A_0(R_b - \delta)] = 0 ,$$

$$\lim_{\delta \rightarrow 0^+} \left[\left(\frac{d}{dr} \delta A_0 \right)_{R_b + \delta} - \left(\frac{d}{dr} \delta A_0 \right)_{R_b - \delta} \right] = 0 . \quad (39)$$

Note from Eqs. (22) and (25) that R_b cannot be evaluated explicitly until $\gamma(r)$ and $\delta A_0(r)$ have been determined from Eqs. (28) and (35), respectively. Furthermore, the solution for $\delta A_0(r)$ depends on R_b . Therefore the condition that determines R_b is, in effect, nonlinear. Introducing the variable ξ defined by

$$\xi = \frac{2\hat{\omega}}{c} pb (rR_c)^{1/2} , \quad (40)$$

the solution to Eq. (28) can be expressed as

$$\gamma(r) = C_1 I_0(\xi) + C_2 K_0(\xi) , \quad (41)$$

within the electron layer. Here, I_n and K_n are modified Bessel functions of order n , and C_1 and C_2 are constants. Eliminating C_1 and C_2 by means of the boundary conditions in Eqs. (31) and (32), it is straightforward to show that Eq. (41) can be expressed as

$$\gamma(r) = \rho [K_1(\rho) I_0(\xi) + I_1(\rho) K_0(\xi)]$$

$$+ 2\alpha [K_0(\rho) I_0(\xi) - I_0(\rho) K_0(\xi)] , \quad (42)$$

where ρ is defined by

$$\rho = \xi(r=R_c) = \frac{2\hat{\omega}}{c} pb R_c . \quad (43)$$

In obtaining Eq. (42), use has been made of the Bessel function identity

$$I_n(z)K_{n+1}(z) + I_{n+1}(z)K_n(z) = 1/z . \quad (44)$$

Similarly, the solution to Eq. (35) can be expressed as

$$\delta A_0(r) = C_3 I_2(\xi) + C_4 K_2(\xi) , \quad (45)$$

for the θ -component of vector potential within the electron layer.

Making use of the recurrence relations for modified Bessel functions,

it is easily shown that

$$\frac{d}{dr} [r\delta A_0(r)] = \frac{\xi}{2} [C_3 I_1(\xi) - C_4 K_1(\xi)] . \quad (46)$$

The coefficients C_3 and C_4 in Eq. (45) are determined from the boundary conditions in Eqs. (37) and (38). After some straightforward algebra, we find that Eq. (45) can be expressed as

$$\delta A_0(r) = R_c B_0 \chi(r) , \quad (47)$$

where the normalized vector potential $\chi(r)$ is

$$\chi(r) = \begin{cases} \frac{2R_b}{na} \frac{K_2(\rho)I_2(\xi) - I_2(\rho)K_2(\xi)}{I_1(\eta)K_2(\rho) + I_2(\rho)K_1(\eta)} , & \text{for } p=+1, \\ 2[K_2(\rho)I_2(\xi) - I_2(\rho)K_2(\xi)] , & \text{for } p=-1. \end{cases} \quad (48)$$

In Eq. (48), the parameter η is defined by

$$\eta = \xi(r=R_b) = \frac{2\hat{\omega}_{pb}}{c} (R_b R_c)^{1/2} = \left(\frac{R_b}{R_c}\right)^{1/2} \rho. \quad (49)$$

In obtaining Eq. (47), use has been made of Eqs. (44) and (46). It is important to note that the variable ξ is restricted to $\xi > \rho$ for $p=+1$, and to $\xi < \rho$ for $p=-1$. Therefore, the normalized vector potential $\chi(r)$ in Eq. (48) satisfies the condition $\chi(r) \geq 0$ for $p=+1$, and $\chi(r) \leq 0$ for $p=-1$, which is consistent with the discussion following Eq. (26).

Making use of Eqs. (22) and (25), the boundary $r=R_b$ of the electron layer is determined from

$$\gamma^2(R_b) - 1 = \frac{\omega_c^2 R_c^2}{c^2} \chi^2(R_b), \quad (50)$$

where the electron cyclotron frequency ω_c at the cathode ($r=R_c$) is defined by

$$\omega_c = eB_0/mc. \quad (51)$$

Once the location of the boundary R_b is determined from Eq. (50), we can also evaluate the electric field at $r=R_b$ from Eq. (42).

Apart from a sign, we define the normalized electric field α_b at $r=R_b$ by

$$\begin{aligned} \alpha_b &= R_b \left(\frac{d\gamma}{dr} \right)_{R_b} = \frac{R_b e}{mc^2} \left[\frac{\partial \phi_0}{\partial r} \right]_{r=R_b} \\ &= \frac{1}{2} n\rho [K_1(\rho) I_1(\eta) - I_1(\rho) K_1(\eta)] \\ &\quad + n\alpha [K_0(\rho) I_1(\eta) + I_0(\rho) K_1(\eta)]. \end{aligned} \quad (52)$$

It is straightforward to show that

$$\gamma(r) = \gamma(R_b) + \alpha_b \ln(r/R_b) , \quad (53)$$

is the solution to the vacuum Poisson equation (29). Evidently, the normalized electric field at $r=R_b$ in Eq. (52) satisfies the condition $\alpha_b \geq 0$ for $p=+1$, and $\alpha_b \leq 0$ for $p=-1$. Making use of Eq. (53), the diode voltage V_0 can be expressed as

$$\frac{eV_0}{mc^2} = \gamma(R_b) - 1 + \begin{cases} \alpha_b \ln(b/R_b) , & \text{for } p=+1 , \\ \alpha_b \ln(a/R_b) , & \text{for } p=-1 . \end{cases} \quad (54)$$

Equations (42), (48), (50), and (54) constitute a complete set of equations which can be used to investigate detailed equilibrium properties for a broad range of physical parameters, including the diode voltage V_0 , the applied magnetic field B_0 , and the conductor radii a and b .

One of the experimentally interesting parameters is the magnetic field at the inner boundary of the electron layer, i.e., $B_{0z}(r=a)$ for $p=+1$, and $B_{0z}(r=R_b)$ for $p=-1$. Evaluating the magnetic field from $B_{0z}(r) = (R_c B_0/r)(d/dr)[r\chi(r)]$, we obtain

$$\begin{aligned} \frac{B_{0z}(a)}{B_0} &= \frac{R_b/a\eta}{K_2(\rho)I_1(\eta)+I_2(\rho)K_1(\eta)} , & \text{for } p=+1 , \\ \frac{B_{0z}(R_b)}{B_0} &= \frac{b\eta}{R_b} [K_2(\rho)I_1(\eta)+I_2(\rho)K_1(\eta)] , & \text{for } p=-1 . \end{aligned} \quad (55)$$

A numerical analysis (Sec. V) confirms that the ratio $B_{0z}(a)/B_0$ in Eq. (55) is less than unity, confirming the "diamagnetic" nature of a diode with positive polarity ($p=+1$ and $R_c=a$). That is, for $r < R_b$,

the magnetic field decreases from the applied value $B_0 = B_{0z}(r=R_b)$ at the outer boundary of the electron layer to the value $B_{0z}(a) < B_0$ at the cathode ($r=a$). On the other hand, $B_{0z}(R_b)/B_0 > 1$ in Eq. (55), indicating the "paramagnetic" nature of a diode with negative polarity ($p=-1$ and $R_c=b$). That is, for $r < b$, the magnetic field increases from the applied value $B_0 = B_{0z}(r=b)$ at the cathode to the value $B_{0z}(R_b) > B_0$ at the inner boundary ($r=R_b$) of the electron layer. Finally, the effective transverse temperature $T_{ib}^0(r)$ is determined by substituting Eqs. (42) and (48) into the expression [Eq. (27)]

$$\frac{T_{ib}^0(r)}{mc^2} = \frac{1}{2} \left[\gamma(r) - \frac{1}{\gamma(r)} - \frac{\omega_c^2 R_c^2}{c^2} \frac{1}{\gamma(r)} \chi^2(r) \right]. \quad (56)$$

IV. PLANAR DIODE EQUILIBRIUM PROPERTIES

In this section, we investigate the equilibrium properties of a magnetically insulated planar diode as the limiting case of a large-aspect-ratio diode with $R_b \gg (b-a)$. In planar geometry,²⁻⁵ the equilibrium distribution function in Eq. (15) is modified to become

$$f_b^0(H, P_y) = \frac{\hat{n}_b}{2\pi m} \delta(H - mc^2) \delta(P_y) , \quad (57)$$

where (x, y) Cartesian coordinates replace the (r, θ) cylindrical polar coordinates in Sec. III, and \hat{n}_b is the electron density at the cathode. Without loss of generality, we assume that the cathode is located at $x=0$ and the anode at $x=d$. The electrons are confined between $x=0$ and $x=x_b$. For planar geometry, Eqs. (28) and (35) become

$$\frac{d^2}{dx^2} \gamma(x) - \frac{\hat{\omega}_p^2}{c^2} \gamma(x) = 0 , \quad (58)$$

$$\frac{d^2}{dx^2} \delta A_0(x) - \frac{\hat{\omega}_p^2}{c^2} \delta A_0(x) = 0 , \quad (59)$$

for $0 \leq x < x_b$, where x_b is the location of the boundary of the electron layer. The electron density profile in Eq. (24) is given by

$$n_b^0(x) = \begin{cases} \gamma(x) \hat{n}_b , & 0 < x < x_b , \\ 0 , & \text{otherwise} , \end{cases} \quad (60)$$

where x_b is determined from

$$[\gamma^2(x_b) - 1] m^2 c^2 = \left[\frac{e}{c} \delta A_0(x_b) \right]^2 . \quad (61)$$

Introducing the electric field parameter defined by

$$\alpha_c = \left(\frac{d\gamma}{dx} \right)_{x=0} = \frac{e}{mc^2} \left(\frac{d\phi_0}{dx} \right)_{x=0}, \quad (62)$$

it is straightforward to show that the solution for $\gamma(x) = 1 + e\phi_0(x)/mc^2$ is

$$\gamma(x) = \begin{cases} \cosh\left(\frac{\hat{\omega}_{pb}x}{c}\right) + \frac{\alpha_c c}{\hat{\omega}_{pb}} \sinh\left(\frac{\hat{\omega}_{pb}x}{c}\right), & 0 \leq x < x_b \\ \cosh\left(\frac{\hat{\omega}_{pb}x_b}{c}\right) + \frac{\alpha_c c}{\hat{\omega}_{pb}} \sinh\left(\frac{\hat{\omega}_{pb}x_b}{c}\right) \\ + \left[\frac{\hat{\omega}_{pb}}{c} \sinh\left(\frac{\hat{\omega}_{pb}x_b}{c}\right) + \alpha_c \cosh\left(\frac{\hat{\omega}_{pb}x_b}{c}\right) \right] (x - x_b), & x_b < x \leq d. \end{cases} \quad (63)$$

The parameter α_c must satisfy $0 \leq \alpha_c < eV_0/mc^2 d$. Moreover, $\alpha_c = 0$ corresponds to space-charge-limited flow with $E_0(x=0)=0$. Enforcing $\gamma(x=d) = 1 + eV_0/mc^2$ at the anode ($x=d$), Eq. (63) gives the condition

$$\frac{eV_0}{mc^2} = \left[\cosh\left(\frac{\hat{\omega}_{pb}x_b}{c}\right) - 1 \right] + \frac{\hat{\omega}_{pb}}{c} \sinh\left(\frac{\hat{\omega}_{pb}x_b}{c}\right) (d - x_b) \\ + \frac{\alpha_c c}{\hat{\omega}_{pb}} \left[\sinh\left(\frac{\hat{\omega}_{pb}x_b}{c}\right) + \frac{\hat{\omega}_{pb}}{c} \cosh\left(\frac{\hat{\omega}_{pb}x_b}{c}\right) (d - x_b) \right], \quad (64)$$

which relates the anode voltage V_0 to the equilibrium parameters x_b , $\hat{\omega}_{pb}$, α_c , and d . Similarly, the y-component of the vector potential $\delta A_0(x)$ is given by

$$\delta A_0(x) = \frac{B_0 c}{\hat{\omega}_{pb}} \frac{\sinh(\hat{\omega}_{pb} x/c)}{\cosh(\hat{\omega}_{pb} x_b/c)}, \quad (65)$$

for $0 \leq x < x_b$. Here, B_0 is the externally applied magnetic field, and use has been made of the boundary conditions, $\delta A_0(x=0) = 0$ and

$[(d/dx)\delta A_0(x)]_{x=x_b} = B_0$. It is useful to evaluate the axial magnetic field at the cathode, i.e.,

$$B_{0z}(0) = \left[\frac{\partial}{\partial x} \delta A_0(x) \right]_{x=0} = B_0 / \cosh(\hat{\omega}_{pb} x_b / c), \quad (66)$$

from Eq. (65). Eliminating B_0 in Eq. (65) in favor of $B_{0z}(0)$, the vector potential $\delta A_0(x)$ can also be expressed as

$$\delta A_0(x) = B_{0z}(0) (c/\hat{\omega}_{pb}) \sinh(\hat{\omega}_{pb} x/c). \quad (67)$$

The effective transverse temperature is determined by substituting Eqs. (63) and (65) into Eq. (27) in the planar limit. After some straightforward algebraic manipulation, the transverse temperature $T_{ib}^0(x)$ can be expressed as

$$T_{ib}^0(x) = \frac{1}{2\gamma(x)} mc^2 \left\{ \frac{1}{\hat{\omega}_{pb}^2} \left[\hat{\omega}_{pb}^2 - \frac{e^2 B_{0z}^2(0)}{m^2 c^2} \right] \sinh^2 \left(\frac{\hat{\omega}_{pb} x}{c} \right) + \alpha_c^2 \frac{c^2}{\hat{\omega}_{pb}^2} \sinh^2 \left(\frac{\hat{\omega}_{pb} x}{c} \right) + \alpha_c \frac{c}{\hat{\omega}_{pb}} \sinh \left(\frac{2\hat{\omega}_{pb} x}{c} \right) \right\}, \quad (68)$$

where $\gamma(x)$ and $B_{0z}(0)$ are given in Eqs. (63) and (66), respectively.

The boundary x_b of the electron layer is determined from

$$\begin{aligned} & \alpha_c^2 \frac{c^2}{\hat{\omega}_{pb}^2} \sinh^2 \left(\frac{\hat{\omega}_{pb} x_b}{c} \right) + \alpha_c \frac{c}{\hat{\omega}_{pb}} \sinh \left(\frac{2\hat{\omega}_{pb} x_b}{c} \right) \\ & = \frac{\omega_c^2}{\hat{\omega}_{pb}^2} \tanh^2 \left(\frac{\hat{\omega}_{pb} x_b}{c} \right) - \sinh^2 \left(\frac{\hat{\omega}_{pb} x_b}{c} \right), \end{aligned} \quad (69)$$

where use has been made of Eqs. (61), (63), and (65). Note from

Eqs. (68) and (69) that the effective transverse temperature vanishes

at $x=x_b$. In general, for arbitrary value of α_c , the inequality

$$\frac{e^2 B_0^2 (0)}{m^2 c^2} \geq \hat{\omega}_{pb}^2, \quad (70)$$

must be satisfied in order to have a nontrivial ($x_b \neq 0$) solution for x_b from Eq. (68).

In the limiting case of space-charge-limited flow²⁻⁵ characterized by $\alpha_c=0$, Eq. (68) reduces to

$$\cosh \left(\frac{\hat{\omega}_{pb} x_b}{c} \right) = \frac{\omega_c}{\hat{\omega}_{pb}}, \quad (71)$$

which also corresponds to

$$\frac{e^2 B_0^2 (0)}{m^2 c^2} = \hat{\omega}_{pb}^2. \quad (72)$$

For space-charge-limited flow, the boundary x_b of the electron layer can be expressed in terms of the externally applied magnetic field B_0 and the plasma frequency $\hat{\omega}_{pb}$ at the cathode by means of Eq. (71). Moreover, these parameters are connected to the anode voltage V_0 by Eq. (64) with $\alpha_c=0$. It is instructive to rewrite Eq. (72) as

$$\left[\frac{e^2 B_0^2 (x)}{\gamma^2 m^2 c^2} \right] \left/ \left[\frac{4\pi e^2 n_b^0 (x)}{\gamma m} \right] \right. = \frac{e^2 B_0^2 (0)}{m^2 c^2 \hat{\omega}_{pb}^2} = 1. \quad (73)$$

That is, the condition for Brillouin flow is satisfied across the entire region where the electron density is non-zero. In obtaining Eq. (73), use has been made of Eqs. (60), (63), and (66). In addition, substituting Eq. (72) into Eq. (68), and taking the limit $\alpha_c=0$, it is found that the

effective transverse temperature $T_{1b}^0(x)$ vanishes for space-charge-limited flow. We therefore conclude that for space-charge-limited flow, a macroscopic cold-fluid model gives an excellent description of the equilibrium properties for monoenergetic electrons. For further discussion of planar diode equilibrium properties in the cold-fluid limit, the reader is referred to Refs. 1 - 5.

In the general case, Eq. (69) can also be expressed as

$$\frac{\alpha_c c}{\hat{\omega}_{pb}} = \left[\coth^2 \left(\frac{\hat{\omega}_{pb} x_b}{c} \right) + \frac{\omega_c^2}{\hat{\omega}_{pb}^2} \operatorname{sech}^2 \left(\frac{\hat{\omega}_{pb} x_b}{c} \right) - 1 \right]^{1/2} - \coth \left(\frac{\hat{\omega}_{pb} x_b}{c} \right), \quad (74)$$

where use has been made of $\alpha_c \geq 0$. For a planar diode, Eqs. (64) and (74) constitute a closed system of equations that can be used to investigate detailed equilibrium properties for various physical parameters, including the diode voltage V_0 , the applied magnetic field B_0 , and the normalized electric field α_c at the cathode. Important equilibrium quantities to be determined from Eqs. (64) and (74) include the location of the boundary x_b of the electron layer, and the electron density ($\hat{\omega}_{pb} d/c$). Shown in Fig. 2(a) are plots of x_b/d versus $\omega_c d/c$ obtained from Eqs. (64) and (74) for $eV_0/mc^2 = 1$ and several values of $\hat{\omega}_{pb} d/c$. The corresponding normalized electric field $\alpha_c d$ at the cathode is plotted versus $\omega_c d/c$ in Fig. 2(b). For low electron density corresponding to $\hat{\omega}_{pb} d/c = 0.6$ in Figs. 2(a) and 2(b), the normalized layer thickness x_b/d decreases monotonically from unity to zero as the applied magnetic field is increased. In this case, the electric field at the cathode (α_c) has a relatively large value [Fig. 2(b)]. For moderate electron density corresponding

to $\hat{\omega}_{pb} d/c = 1.2$ in Figs. 2(a) and 2(b), there are two solutions for the normalized layer thickness x_b/d and the normalized electric field $\alpha_c d$ at the cathode that satisfy Eqs. (64) and (74) over a portion of the range of $\omega_c d/c$. For specified beam density and applied magnetic field, the thick-layer equilibrium solution corresponds to weak electric field at the cathode, and the thin-layer equilibrium solution corresponds to strong electric field at the cathode. For example, for $\hat{\omega}_{pb} d/c = 1.2$ and $\alpha_c d/c = 2.3$ in Figs. 2(a) and 2(b), the solution $x_b/d = 0.4$ corresponds to $\alpha_c d = 0.48$, whereas the solution $x_b/d = 0.9$ corresponds to $\alpha_c d = 0.17$. It is evident from Figs. 2(a) and 2(b) that high electron density occurs for relatively small values of electric field at the cathode. For $\hat{\omega}_{pb} d/c = 1.8$ in Fig. 2(b), the electric field at the cathode vanishes ($\alpha_c = 0$) for $\omega_c d/c = 2.18$, and the layer thickness is given by $x_b/d = 0.35$. This corresponds to space-charge-limited flow with $E_{0x}(x=0) = 0$.

Shown in Fig. 2(c) are plots of x_b/d versus $\omega_c d/c$ obtained from Eqs. (64) and (74) for $eV_0/mc^2 = 1$ and several values of $\alpha_c d$. The corresponding values of $\hat{\omega}_{pb} d/c$ are plotted in Fig. 2(d). What is remarkable in Fig. 2(c) is that there are two solutions for the normalized layer thickness x_b/d that satisfy Eqs. (64) and (74) over a portion of the range of $\omega_c d/c$. For example, for space-charge-limited flow characterized by $\alpha_c = 0$ in Figs. 2(c) and 2(d), the quantities x_b/d and $\hat{\omega}_{pb} d/c$ have two solutions when the applied magnetic field is in the range $2.1 < \omega_c d/c < 2.575$. For the case of space-charge-limited flow in Fig. 2(c), the minimum value of magnetic field required for the equilibrium to exist is determined from $eB_{\min} d/mc^2 = 2.1$. That is, equilibrium solutions do not exist for $\alpha_c = 0$ and $B_0 < B_{\min}$. Although for space-charge-limited flow there are two distinct solutions for x_b/d when $\omega_c d/c$

is in the range $2.1 < \omega_c d/c < 2.575$, the thick-layer equilibrium solution in the range of $0.5 < x_b/d < 1$ is likely to be unattainable. In a typical experimental application, the electrons are initially emitted from the cathode with electric field in the gap, $E_0 = -V_0/d$, corresponding to $\alpha_c d = eV_0/mc^2$. Therefore, in time sequence, the system is expected to evolve from a quasi-equilibrium state with $\alpha_c d = eV_0/mc^2$ to one with $\alpha_c d = 0$ for a specified value of applied magnetic field B_0 . For example, for $\omega_c d/c = 2.3$ in Figs. 2(c), the layer thickness x_b/d would evolve from $x_b/d \approx 0.5$ (corresponding to $\alpha_c d = eV_0/mc^2 = 1$) to $x_b/d = 0.3$ (corresponding to $\alpha_c d = 0$). In this regard, the thin-layer equilibrium solution in Fig. 2(c) appears to be the physically acceptable solution. Finally, it should also be noted from Fig. 2(d) that the normalized electron density ($\hat{\omega}_{pb} d/c$) increases rapidly with decreasing value of electric field at the cathode ($\alpha_c d$).

V. CYLINDRICAL DIODE EQUILIBRIUM PROPERTIES

In this section, the equilibrium properties of a nonneutral electron layer confined in a magnetically insulated cylindrical diode are determined numerically from Eqs. (42), (48), (50) and (54) for a broad range of system parameters including diode voltage V_0 , externally applied magnetic field B_0 , and conductor radii a and b . Important equilibrium quantities include the radial location of the boundary R_b of the electron layer, the electron density profile $n_b^0(r)$, and the axial magnetic field and transverse temperature profiles.

A. Positive Polarity Diode

In this section, we investigate numerically the equilibrium properties of a magnetically insulated diode with positive polarity ($p=+1$ and $R_c=a$). For a specified value of electron density at the cathode, i.e., $\hat{\omega}_{pb}^2 a^2/c^2$, the relativistic mass factor $\gamma(r)$ and the axial component of vector potential $\delta A_0(r)$ are calculated from Eqs. (42) and (48). Substituting the resulting profiles for $\gamma(r)$ and $\delta A_0(r)$ into Eq. (50), we can determine the plasma boundary R_b for a given value of $\omega_c^2 a^2/c^2$. Once the location of the boundary R_b is calculated, the electron density profile $n_b^0(r)$, the azimuthal velocity profile $V_{\theta b}^0(r)$, and the axial magnetic field $B_{0z}(r)$ are obtained from Eqs. (24), (26), and $B_{0z}(r) = (aB_0/r)(d/dr)[rX(r)]$, respectively. Shown in Fig. 3 are the radial profiles for (a) $n_b^0(r)$, and (b) $V_{\theta b}^0(r)$ and $B_{0z}(r)$, for the choice of parameters $\hat{\omega}_{pb}^2 a^2/c^2 = 3$, $b/a = 2$, $eV_0/mc^2 = 0.792$, and $\omega_c^2 a^2/c^2 = 7$, assuming space-charge-limited flow with $\alpha = 0$.

As indicated in the discussion following Eq. (26), the azimuthal velocity $V_{\theta b}^0(r)$ in Fig. 3(b) is in the positive θ -direction, which gives a diamagnetic depression in the axial magnetic field. Indeed, the axial magnetic

field at the cathode, $B_{0z}(r=a)$ is depressed considerably relative to the vacuum value B_0 for the choice of parameters in Fig. 3. We also find from the numerical analysis that the effective transverse temperature $T_{\perp b}^0(r)$ in Eq. (56) is negligibly small for space-charge-limited flow ($\alpha=0$) in a diode with positive polarity. Shown in Fig. 4 are plots of the normalized boundary location R_b/a versus $\omega_c^2 a^2/c^2$ for $\alpha=0$ and several values of $\hat{\omega}_{pb}^2 a^2/c^2$. It is evident from Fig. 4 that confinement of a dense electron layer requires a strong applied magnetic field B_0 . Substituting the value obtained for R_b in Fig. 4 into Eq. (55), we can also determine the magnetic field at the cathode $B_{0z}(a)$ for specified values of $\hat{\omega}_{pb}^2 a^2/c^2$ and $\omega_c^2 a^2/c^2$.

Of considerable practical interest are the equilibrium properties of the electron layer for specified values of b/a , diode voltage V_0 , and applied magnetic field B_0 . Typical results are shown in Fig. 5, where (a) R_b/a , and (b) $\hat{\omega}_{pb}^2 a^2/c^2$ are plotted versus $\omega_c^2 a^2/c^2$ for $b/a=2$, $\alpha=0$ and several values of eV_0/mc^2 . As expected, the thickness of the electron layer decreases significantly as the applied magnetic field B_0 is increased for specified diode voltage V_0 . Moreover, for each value of V_0 , there is a minimum value of applied magnetic field B_0 required for insulation of the electron flow from contact with the anode. For example, for $eV_0/mc^2=0.3$ in Fig. 5(a), the minimum magnetic field B_{\min} is determined from $\omega_c^2 a^2/c^2=1.25$. For $B_0 > B_{\min}$, the electron layer is confined in the diode with $R_b < b$, and the electron flow is insulated from contact with the anode. For $B_0 < B_{\min}$, however, the applied magnetic field is not sufficiently strong to insulate the electron flow from contact with the anode. It is evident from Fig. 5(a) that the minimum field B_{\min} required for magnetic insulation increases with increasing value of the diode voltage V_0 . Although the

layer thickness R_b - a decreases with increasing magnetic field B_0 , it follows from Fig. 5(b) that the electron density ($\hat{\omega}_{pb}^2 a^2/c^2$) increases with increasing B_0 for a specified value of diode voltage V_0 .

In order to demonstrate the influence of non-zero electric field at the cathode ($\alpha \neq 0$) on diode equilibrium properties, shown in Fig. 6 is a plot of the transverse temperature profile $T_{\perp b}^0(r)$ for $b/a = 2$, $\hat{\omega}_{pb}^2 a^2/c^2 = 3$, and several values of the diode voltage V_0 and cathode electric field parameter α defined in Eq. (32). A large cathode electric field requires high applied magnetic field B_0 to assure insulated electron flow. In order to fix the layer boundary at $R_b/a = 1.7$ in Fig. 6, for each value of α we have varied the diode voltage V_0 and the applied magnetic field B_0 . In Fig. 6, the values are $(\alpha, eV_0/mc^2, \omega_c^2 a^2/c^2) = (0, 0.79, 7), (0.1, 0.87, 8), (0.2, 0.95, 9.03), (0.3, 1.03, 10.1)$ and $(0.4, 1.11, 11.22)$. For space-charge-limited flow with $\alpha = 0$, it is evident from Fig. 6 that the transverse temperature $T_{\perp b}^0(r)$ is negligibly small. However, increasing the value of α can significantly increase the transverse temperature $T_{\perp b}^0(r)$ (Fig. 6), and the corresponding r - z motion of the electrons. Also tabulated in Fig. 6 is the relativistic mass factor $\gamma_b \equiv \gamma(R_b)$ at the surface of the electron layer. It is evident from Fig. 6, that $\gamma_b = \gamma(R_b)$ increases with increasing values of α .

In Fig. 7, we investigate equilibrium properties for specified values of b/a and diode voltage V_0 . Shown in Fig. 7 are plots of (a) R_b/a , (b) $\hat{\omega}_{pb}^2 a^2/c^2$, and (c) $B_{0z}(a)/B_0$ versus $\omega_c^2 a^2/c^2$, for $b/a = 2$, $eV_0/mc^2 = 0.5$, and several values of α . It is clear from Fig. 7(a) that the location of the layer boundary R_b exhibits only a weak dependence on the electric field strength at the cathode as measured by the parameter α . In contrast with the behavior of R_b/a shown in Fig. 7(a), the normalized electron density

$\hat{\omega}_{pb}^2 a^2/c^2$ plotted in Fig. 7(b) varies rapidly with the electric field at the cathode. It is evident from Fig. 7(b) that the electron density decreases rapidly with increasing values of α . Once the values of R_b and $\hat{\omega}_{pb}^2$ are determined, we can calculate the axial magnetic field at the cathode $B_{0z}(a)$ from Eq. (55). Shown in Fig. 7(c) are plots of $B_{0z}(a)/B_0$ versus $\omega_c^2 a^2/c^2$ for $\alpha=0$ and $\alpha=0.2$. The axial magnetic field at the cathode decreases substantially as the applied magnetic field approaches the minimum value, $\omega_c^2 a^2/c^2 \approx 2.5$, required for magnetic insulation. (In this limit, the electron layer fills the entire diode region.) Note from Fig. 7(c) that $B_{0z}(a)/B_0$ is only weakly dependent on α .

B. Negative Polarity

The electron layer in a magnetically insulated diode with negative polarity ($p=-1$ and $R_c=b$) exhibits paramagnetic equilibrium properties. For negative polarity, we remind the reader that the cathode is located at the outer conductor with $\phi_0(r=b)=0$, and the anode is located at the inner conductor with $\phi_0(r=a)=V_0$. Equilibrium properties are calculated numerically from Eqs. (42), (48), (50) and (54). Typical numerical results are summarized in Fig. 8, where (a) $n_b^0(r)$ and $T_{\perp b}^0(r)$, and (b) $B_{0z}(r)$ and $V_{\theta b}^0(r)$ are plotted versus r/b for $\alpha=0$, $b/a=2$, $eV_0/mc^2=0.694$, $\hat{\omega}_{pb}^2 b^2/c^2=3$, and $\omega_c^2 b^2/c^2=2.5$. In contrast to the case with positive polarity, it is found that the transverse temperature for space-charge-limited flow ($\alpha=0$) in a diode with negative polarity is not negligibly small. We also emphasize that the azimuthal velocity of an electron fluid element is in the negative θ -direction, consistent with the paramagnetic nature of the equilibrium [Fig. 8(b)]. In this regard, the axial magnetic field at the anode $B_{0z}(a)$ [evaluated from Eq. (55)] is significantly larger than the applied field $B_0=B_{0z}(b)$ [Fig. 8(b)]. Shown in Fig. 9 are plots of R_b/b

versus $\omega_c^2 b^2 / c^2$ for $\alpha = 0$, and several values of $\hat{\omega}_{pb}^2 b^2 / c^2$. The plasma thickness decreases rapidly with increasing $\omega_c^2 b^2 / c^2$ and fixed value of $\hat{\omega}_{pb}^2 b^2 / c^2$. This property is considerably enhanced by the paramagnetic nature of the equilibrium at moderately large electron density. Once the boundary location R_b is determined in terms of $\hat{\omega}_{pb}^2$ and ω_c from Fig. 9, we can obtain all of the necessary equilibrium quantities from Eqs. (54) and (55).

Shown in Fig. 10 are plots of (a) R_b/b , (b) $\hat{\omega}_{pb}^2 b^2 / c^2$, and (c) $B_{0z}(a)/B_0$ versus $\omega_c^2 b^2 / c^2$ for the space-charge-limited flow with $\alpha = 0$, $a/b = 0.5$, and several values of the normalized diode voltage eV_0/mc^2 . From Fig. 10(a), we find that high diode voltage V_0 requires a strong applied magnetic field B_0 for magnetic insulation of the electron flow from contact with the anode at $r = a$. The minimum magnetic field required for insulation also increases with diode voltage. It is interesting to compare Fig. 5(a) with Fig. 10(a). The minimum magnetic field B_{min} required for magnetic insulation in a negative polarity diode is much less than that required for a positive polarity diode. The reason for the smaller value of B_{min} is associated with the paramagnetic nature of the electron layer in a negative polarity diode. From Fig. 10(b), it is quite remarkable that the electron density is relatively insensitive to the diode voltage V_0 . However, high electron density requires relatively high applied magnetic field for confinement of the electrons. Substituting the values obtained for R_b/b and $\hat{\omega}_{pb}^2 b^2 / c^2$ in Eq. (55) determines the axial magnetic field at the anode ($r = a$). Note that $B_{0z}(R_b) = B_{0z}(a)$ for $p = -1$. Shown in Fig. 10(c) are plots of $B_{0z}(a)/B_0$ versus $\omega_c^2 b^2 / c^2$. The axial magnetic field at the anode increases substantially whenever the applied magnetic field B_0 approaches the minimum value B_{min} required for magnetic insulation. In general, higher diode voltages exhibits a more enhanced increase in $B_{0z}(a)$ because of the higher density of the electron layer.

The influence of non-zero electric field at the cathode ($\alpha \neq 0$) on equilibrium properties is illustrated in Fig. 11 where the transverse temperature $T_{\perp b}^0(r)$ is plotted versus r/b for $\hat{\omega}_{pb}^2 b^2/c^2 = 3$, $b/a = 2$, $R_b/b = 0.66$, and several values of α . For $R_b/b = 0.66$, the self-consistent values of α , eV_0/mc^2 , and $\omega_c^2 b^2/c^2$ in Fig. 11 are given by $(\alpha, eV_0/mc^2, \omega_c^2 b^2/c^2) = (0, 0.69, 2.5)$, $(-0.1, 0.79, 3.03)$, $(-0.2, 0.89, 3.59)$, $(-0.3, 0.98, 4.16)$ and $(-0.4, 1.08, 4.79)$. Note that the values of α are negative for a negative polarity diode with $p = -1$. In contrast with Fig. 6, the transverse temperature for space-charge-limited flow ($\alpha = 0$) in a negative polarity diode is not negligibly small. Also shown in Fig. 11 are the values of $\gamma_b = \gamma(R_b)$ at the layer boundary R_b for different values of α . Evidently, γ_b increases for increasing values of $|\alpha|$. The dependence of the location of the layer boundary R_b on the electric field at the cathode is illustrated in Fig. 12 where R_b/b is plotted versus $\omega_c^2 b^2/c^2$ for $\hat{\omega}_{pb}^2 b^2/c^2 = 3$ and several values of α . It is evident from Fig. 12 that increasing the parameter $|\alpha|$ requires stronger applied magnetic field B_0 in order to confine the electron layer.

Finally, in Fig. 13, we plot (a) R_b/b and (b) $\hat{\omega}_{pb}^2 b^2/c^2$ versus $\omega_c^2 b^2/c^2$ for normalized diode voltage $eV_0/mc^2 = 0.7$, $a/b = 0.5$, and several values of α . It is evident from Fig. 13(a) that the location of the layer boundary R_b is weakly dependent on the parameter α . However, larger values of $|\alpha|$ requires stronger magnetic field B_0 to confine the electron layer. From Fig. 13(b), for fixed $\omega_c^2 b^2/c^2$, the normalized electron density $\hat{\omega}_{pb}^2 b^2/c^2$ decreases as $|\alpha|$ is increased. From the numerical calculations for $\alpha \neq 0$ we find that the axial magnetic field at the anode $B_{0z}(a)$ is almost identical to that obtained for space-charge-limited flow ($\alpha = 0$) in Fig. 10(c).

VI. CONCLUSIONS

In this paper we have investigated the equilibrium properties of a relativistic nonneutral electron layer confined in a magnetically insulated cylindrical diode within the framework of the steady-state ($\partial/\partial t=0$) Vlasov-Maxwell equations. The analysis was carried out for an infinitely long electron layer aligned parallel to a uniform applied magnetic field $B_0 \hat{e}_z$, which radially insulates the electron flow from contact with the anode. The theoretical model and basic assumptions were discussed in Sec. II, allowing for both polarities of the electric field. Also discussed in Sec. II was the general formalism for describing equilibrium properties within the framework of the steady-state Vlasov-Maxwell equations. In Sec. III, we specialized to the class of self-consistent Vlasov equilibria in which all electrons have the same canonical angular momentum ($P_\theta = P_0 = \text{const.}$) and the same energy ($H = mc^2$). One of the most important results in this analysis is that closed analytic expressions are obtained for the self-consistent electrostatic potential and the θ -component of vector potential. Moreover, the various equilibrium properties of physical interest can be calculated readily from these potentials. As a special limiting case, in Sec. IV we investigated the detailed equilibrium properties of a magnetically insulated planar diode. One of the important features of the analysis in Sec. IV is that the transverse temperature $T_{\perp b}^0(x)$ vanishes identically for space-charge-limited flow with zero electric field at the cathode.

In Sec. V, the detailed equilibrium properties of a cylindrical diode were investigated over a broad range of system parameters, including diode voltage V_0 , cathode electric field (α), electron density \hat{n}_b at the cathode,

applied magnetic field B_0 , and the ratio b/a of the inner and outer conductor radii. Several features of the analysis are noteworthy. First, the electron layer in a positive polarity diode exhibits diamagnetic behavior, whereas the electron layer in a negative polarity diode exhibits paramagnetic properties. Indeed, a negative polarity diode is more effective in confining the electrons because the magnetic field in the anode region is larger than the externally applied magnetic field B_0 . Second, the layer thickness decreases with increasing applied magnetic field B_0 . However, the layer thickness is an increasing function of diode voltage V_0 . Third, the density of the electron layer increases with applied magnetic field B_0 . Fourth, the transverse temperature $T_{\perp b}^0(r)$ increases substantially as the strength of the electric field at the cathode is increased. We therefore find that the density of the electron layer decreases as the electric field at the cathode is increased.

ACKNOWLEDGMENTS

This research was supported by Sandia National Laboratories and in part by the Office of Naval Research.

REFERENCES

1. R.C. Davidson and K.T. Tsang, Phys. Rev. A29, 488 (1984).
2. R.C. Davidson, K.T. Tsang and J.A. Swegle, Phys. Fluids 27, 2332 (1984).
3. J. Swegle, Phys. Fluids 26, 1670 (1983).
4. J. Swegle and E. Ott, Phys. Fluids 24, 1821 (1981).
5. J. Swegle and E. Ott, Phys. Rev. Lett. 46, 929 (1981).
6. R.C. Davidson, "Quasilinear Theory of Diocotron Instability for Nonrelativistic Nonneutral Electron Flow in Planar Diode with Applied Magnetic Field," submitted for publication (1984).
7. R.C. Davidson, Phys. Fluids 27, in press (1984).
8. J.P. VanDevender, J.P. Quintenz, R.J. Leeper, D.J. Johnson and J.T. Crow, J. Appl. Phys. 52, 4 (1981).
9. R.B. Miller, Intense Charged Particle Beams (Plenum, New York, 1982).
10. O. Buneman, Proc. Cambridge Phil. Soc. 50, 77 (1954).
11. R.H. Levy, Phys. Fluids 8, 1288 (1965).
12. O. Buneman, R.H. Levy and L.M. Linson, J. Appl. Phys. 37, 3203, (1966).
13. R.J. Briggs, J.D. Daugherty and R.H. Levy, Phys. Fluids 13, 421, (1970).
14. C.A. Kapetanakis, D.A. Hammer, C.D. Striffler and R.C. Davidson, Phys. Rev. Lett. 30, 1303 (1973).
15. R.C. Davidson, Theory of Nonneutral Plasmas (Benjamin, Reading, Mass., 1974) pp. 17-89.
16. V.S. Voronen and A.N. Lebedev, Zh. Tekh. Fiz. 43, 2591 (1973) [Sov. Phys.-Tech. Phys. 18, 1627 (1974)].
17. E. Ott and R.V. Lovelace, Appl. Phys. Lett. 27, 378 (1975).
18. R.C. Davidson, Ref. 15, pp. 90-177.
19. R.C. Davidson, S.M. Mahajan and H.S. Uhm, Phys. Fluids 19, 1608 (1976).
20. H.S. Uhm and R.C. Davidson, Phys. Fluids 20, 771 (1977).
21. A. Nocentini, H.L. Berk and R.N. Sudan, J. Plasma Phys. 2, 311 (1968).

FIGURE CAPTIONS

- Fig. 1 Cylindrical diode configuration. Equilibrium electron flow is in the θ -direction. The boundary of the electron layer is denoted by R_b , and the applied plus self magnetic field $B_0(x) = (B_0 + B_{0z}^s)\hat{e}_z$ is in the z -direction.
- Fig. 2 Plots of (a) the normalized boundary location x_b/d and (b) $\alpha_c d$ versus $\omega_c d/c$ obtained from Eqs. (64) and (74) for $eV_0/mc^2 = 1$ and several values of $\hat{\omega}_{pb} d/c$. Also shown are plots of (c) x_b/d and (d) $\hat{\omega}_{pb} d/c$ versus $\omega_c d/c$ for $eV_0/mc^2 = 1$ and several values of normalized electric field $\alpha_c d$ at the cathode.
- Fig. 3 Radial profiles of (a) electron density $n_b^0(r)$, and (b) $V_{\theta b}^0(r)$ and $B_{0z}(r)$ for $\hat{\omega}_{pb}^2 a^2/c^2 = 3$, $\omega_c^2 a^2/c^2 = 7$, $b/a = 2$, $eV_0/mc^2 = 0.79$, $\alpha = 0$, and $p = +1$.
- Fig. 4 Plots of normalized location of the layer boundary R_b/a versus $\omega_c^2 a^2/c^2$ for $\alpha = 0$, $p = +1$, and several values of $\hat{\omega}_{pb}^2 a^2/c^2$.
- Fig. 5 Plots of (a) R_b/a , and (b) $\hat{\omega}_{pb}^2 a^2/c^2$ versus $\omega_c^2 a^2/c^2$ for $b/a = 2$, $\alpha = 0$, $p = +1$, and several values of normalized diode voltage eV_0/mc^2 .
- Fig. 6. Profiles of the transverse temperature $T_{\perp b}^0(r)$ for $p = +1$, $b/a = 2$, $\hat{\omega}_{pb}^2 a^2/c^2 = 3$, and several values of normalized cathode electric field α . In order to maintain the same value of $R_b/a = 1.7$, the applied magnetic field ($\omega_c^2 a^2/c^2$) and diode voltage (eV_0/mc^2) are adjusted accordingly for each value of α .

- Fig. 7 Plots of (a) R_b/a , (b) $\hat{\omega}_{pb}^2 a^2/c^2$, and (c) $B_{0z}(a)/B_0$ versus $\omega_c^2 a^2/c^2$ for $p=+1$, $b/a=2$, $eV_0/mc^2=0.5$, and several values of α .
- Fig. 8 Profiles of (a) $n_b^0(r)$ and $T_{\perp b}^0(r)$, (b) $B_{0z}(r)$ and $V_{\theta b}^0(r)$ for $a/b=0.5$, $p=-1$, $\alpha=0$, $\hat{\omega}_{pb}^2 b^2/c^2=3$, $\omega_c^2 b^2/c^2=2.5$, and $eV_0/mc^2=0.694$.
- Fig. 9 Plots of the normalized boundary location R_b/b versus $\omega_c^2 b^2/c^2$ for $p=-1$, $\alpha=0$, and several values of $\hat{\omega}_{pb}^2 b^2/c^2$.
- Fig. 10 Plots of (a) R_b/b , (b) $\hat{\omega}_{pb}^2 b^2/c^2$, and (c) $B_{0z}(a)/B_0$ versus $\omega_c^2 b^2/c^2$ for $\alpha=0$, $p=-1$, $a/b=0.5$, and several values of normalized diode voltage eV_0/mc^2 .
- Fig. 11 Profiles of the transverse temperature $T_{\perp b}^0(r)$ for $p=-1$, $a/b=0.5$, $R_b/b=0.66$, $\hat{\omega}_{pb}^2 b^2/c^2=3$, and several self-consistent values of $(\alpha, eV_0/mc^2, \omega_c^2 b^2/c^2)$.
- Fig. 12 Plots of the normalized boundary location R_b/b versus $\omega_c^2 b^2/c^2$ for $p=-1$, $\hat{\omega}_{pb}^2 b^2/c^2=3$, and several values of α .
- Fig. 13 Plots of (a) R_b/b , and (b) $\hat{\omega}_{pb}^2 b^2/c^2$ versus $\omega_c^2 b^2/c^2$ for $p=-1$, $a/b=0.5$, $eV_0/mc^2=0.7$, and several values of α .

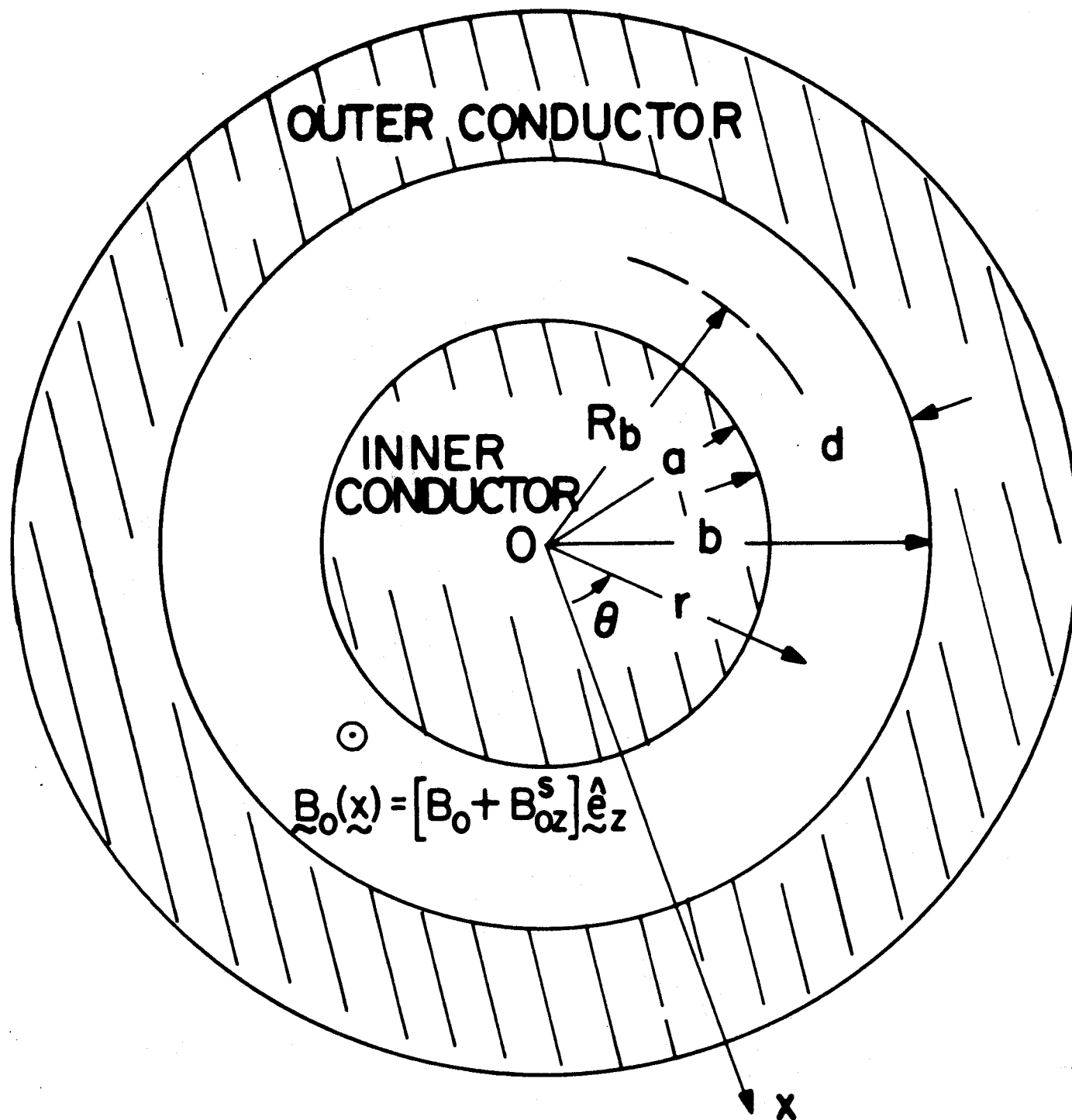


Fig. 1

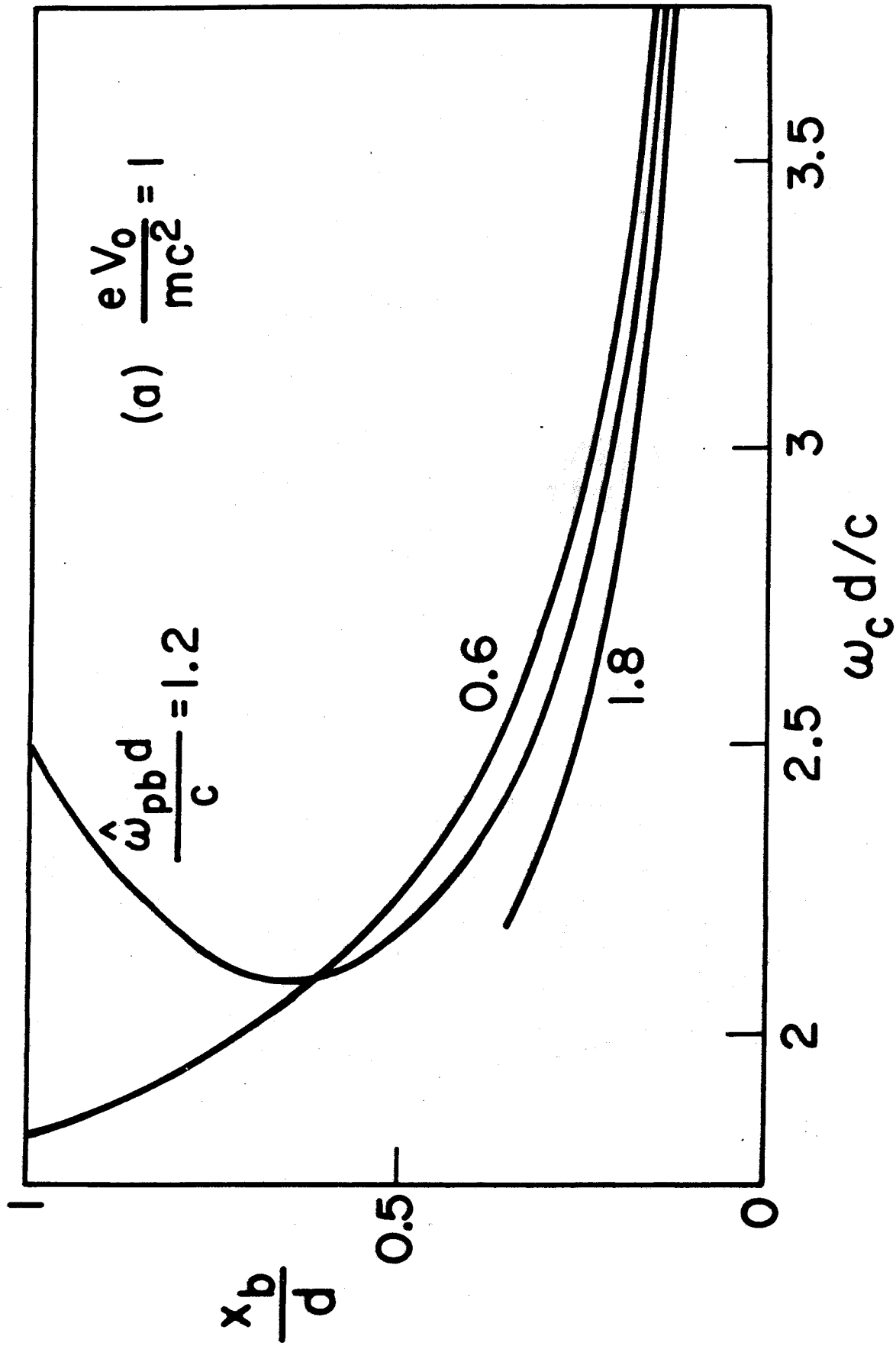


Fig. 2(a)

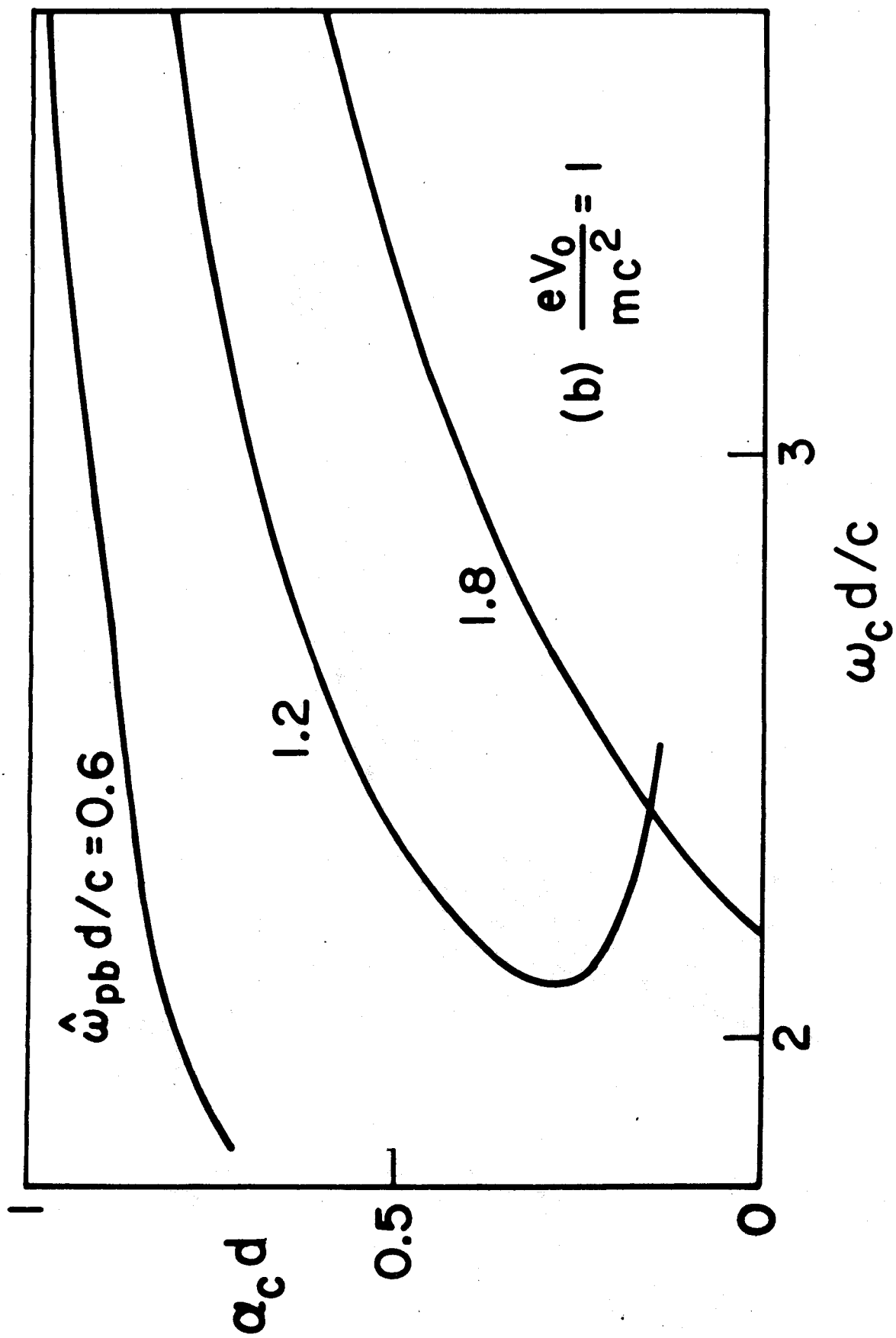


Fig. 2(b)

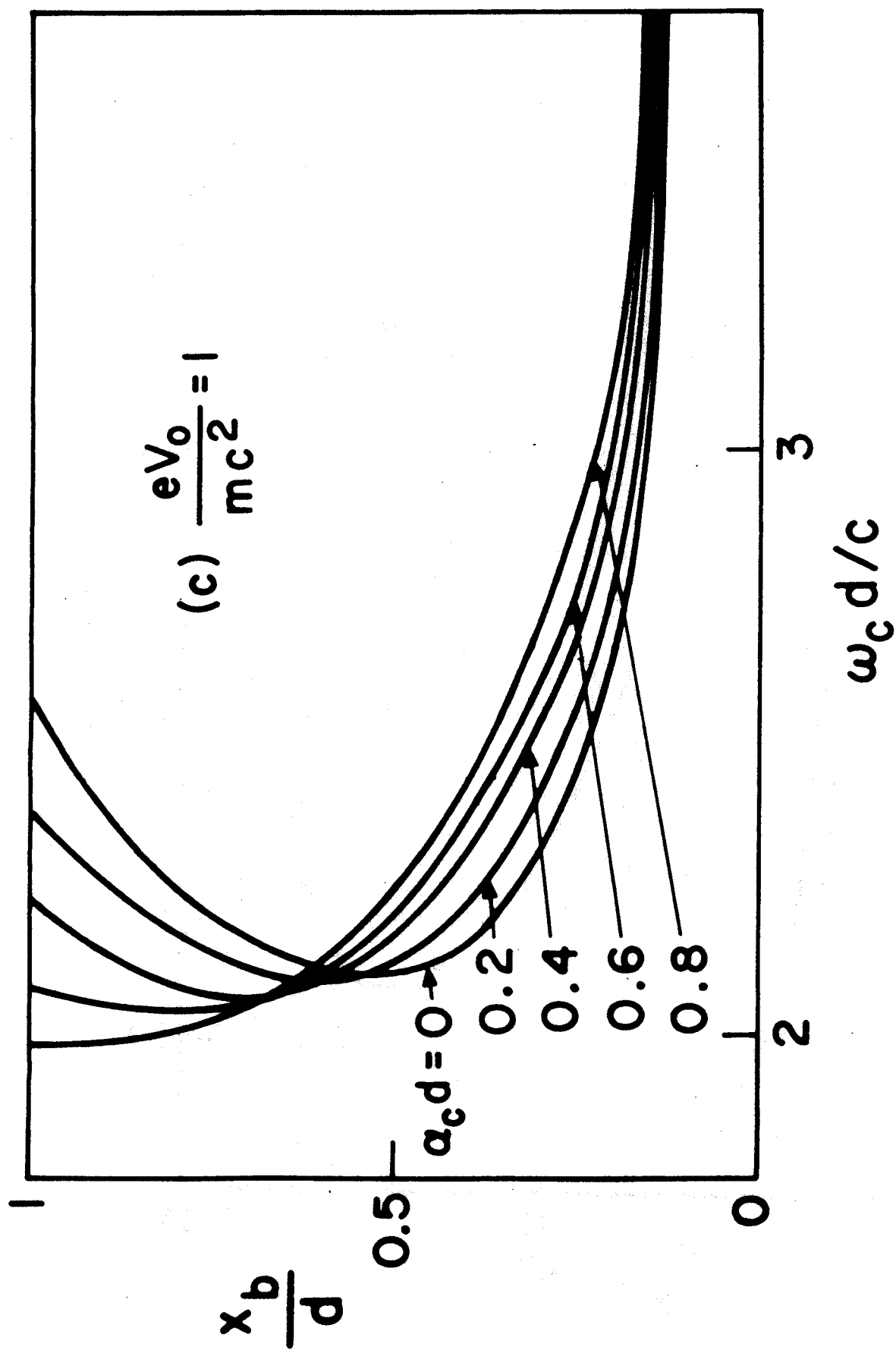


Fig. 2(c)

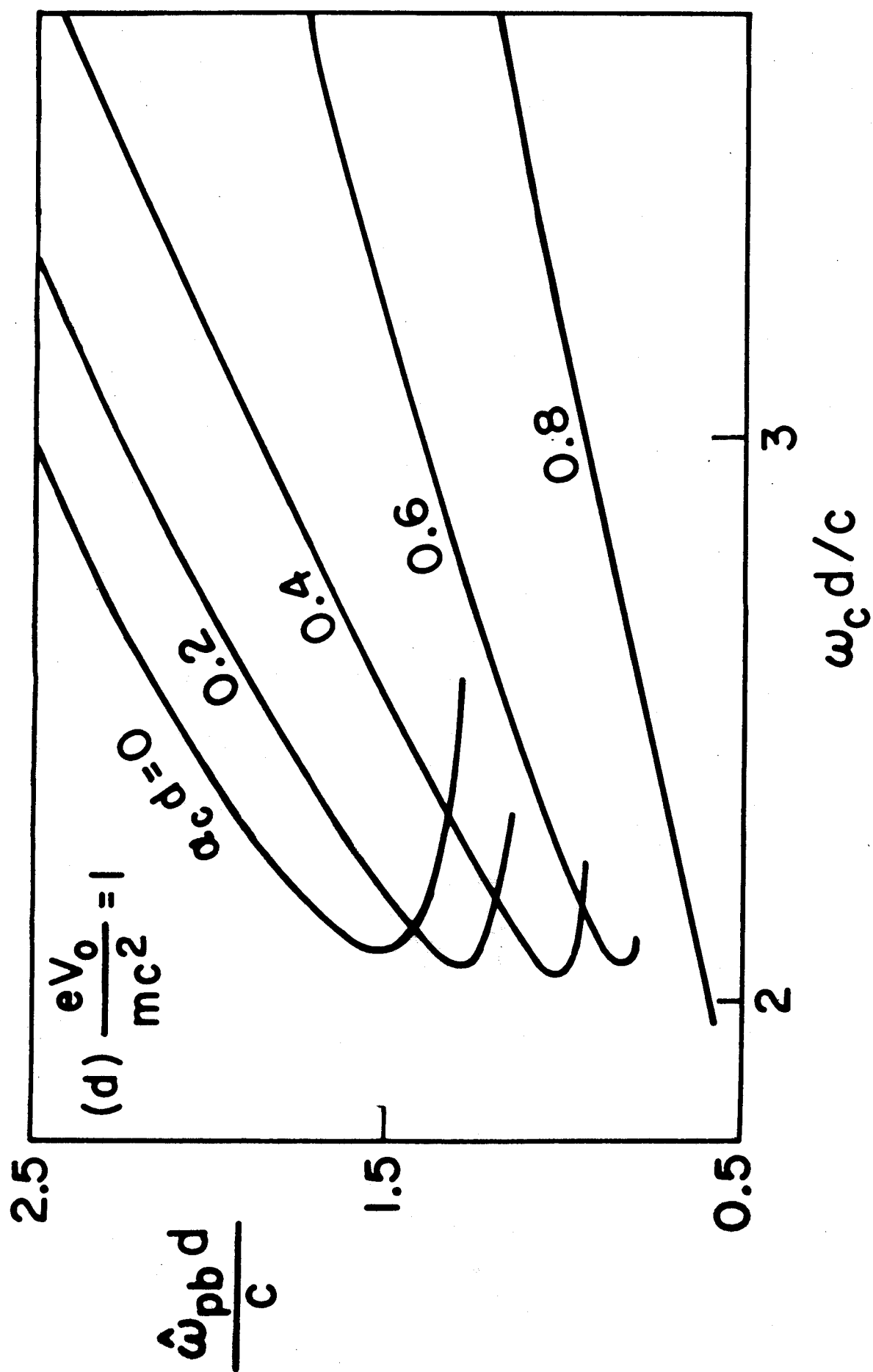


Fig. 2(d)

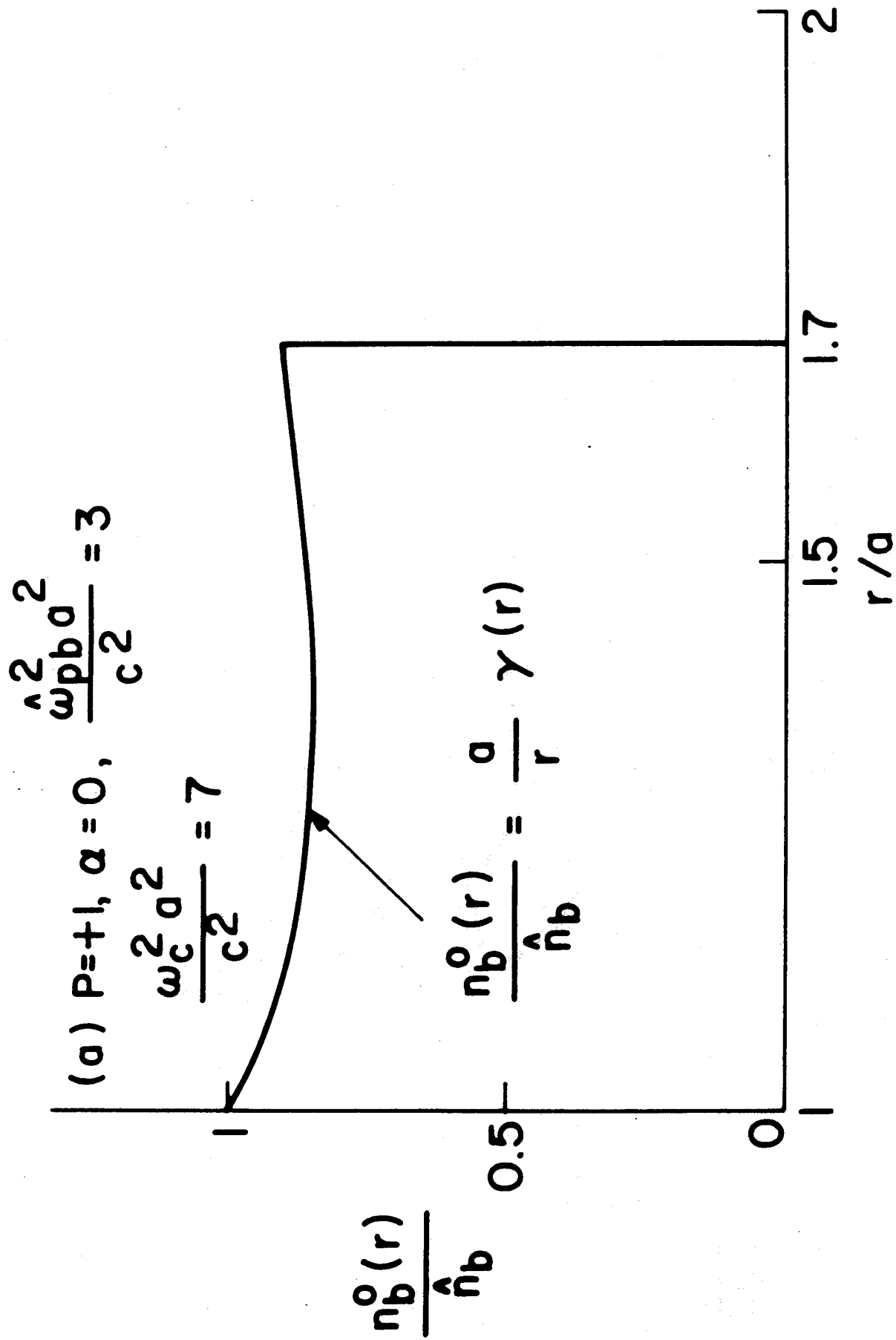


Fig. 3(a)

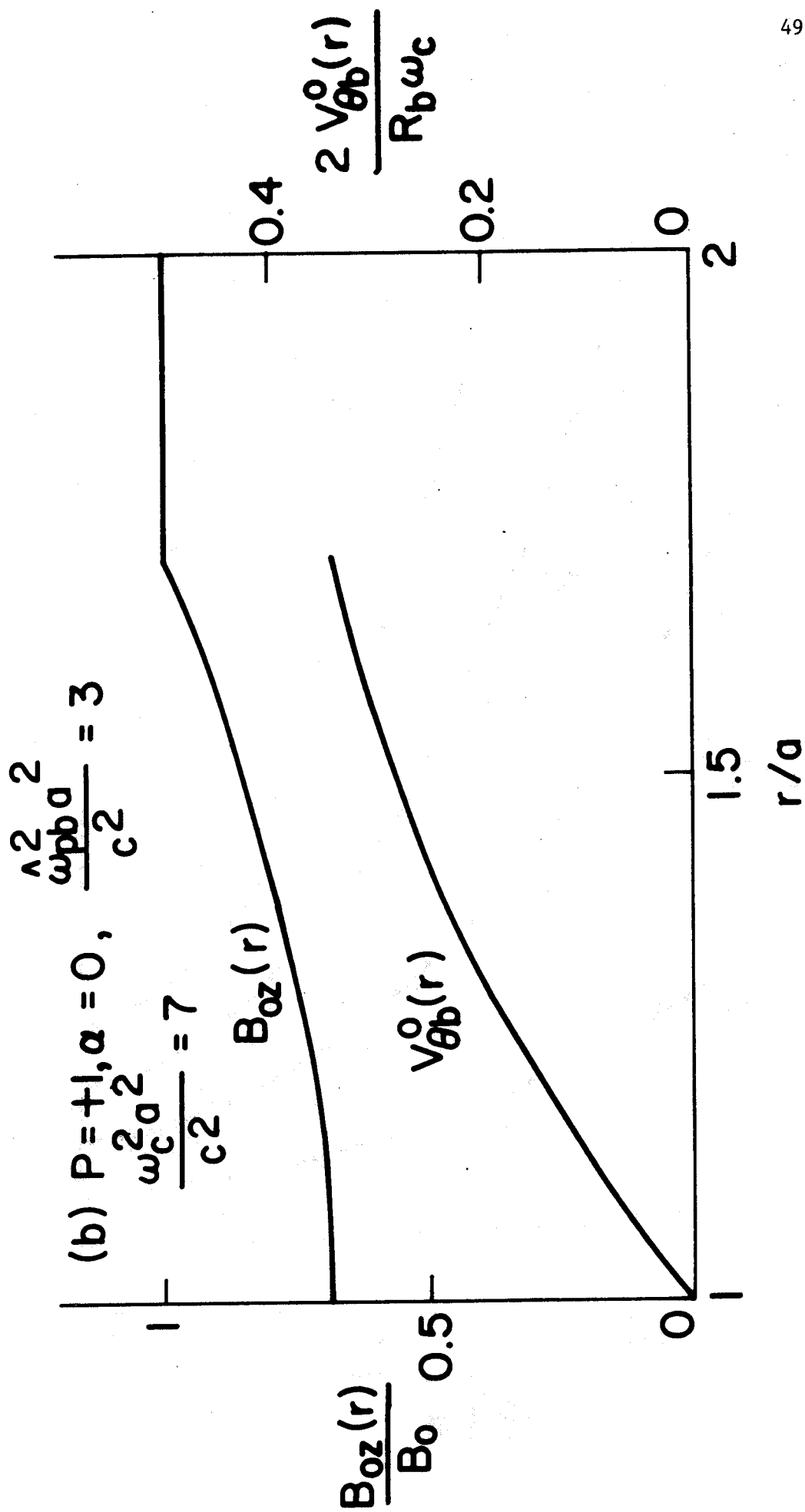


Fig. 3(b)

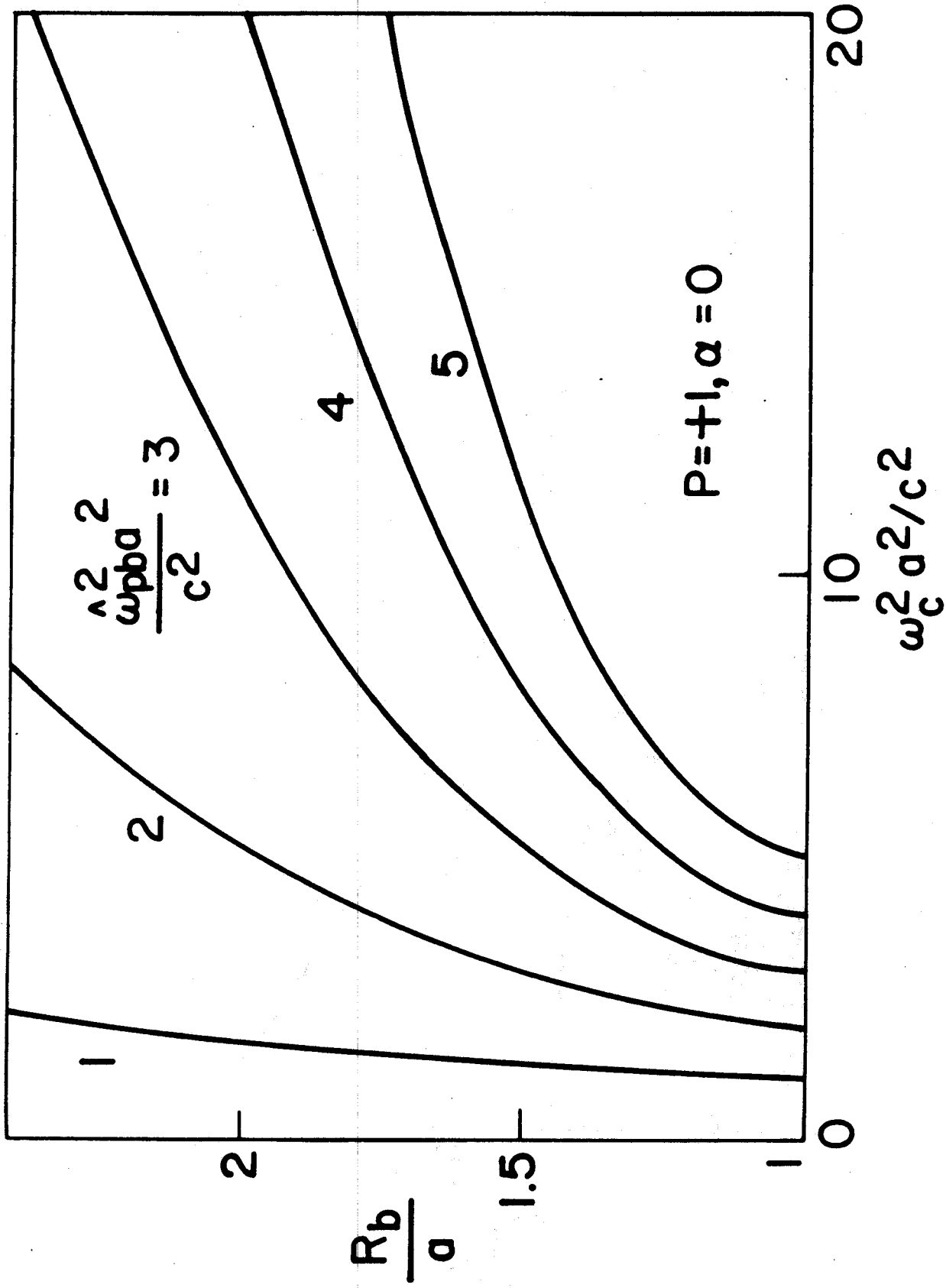


Fig. 4

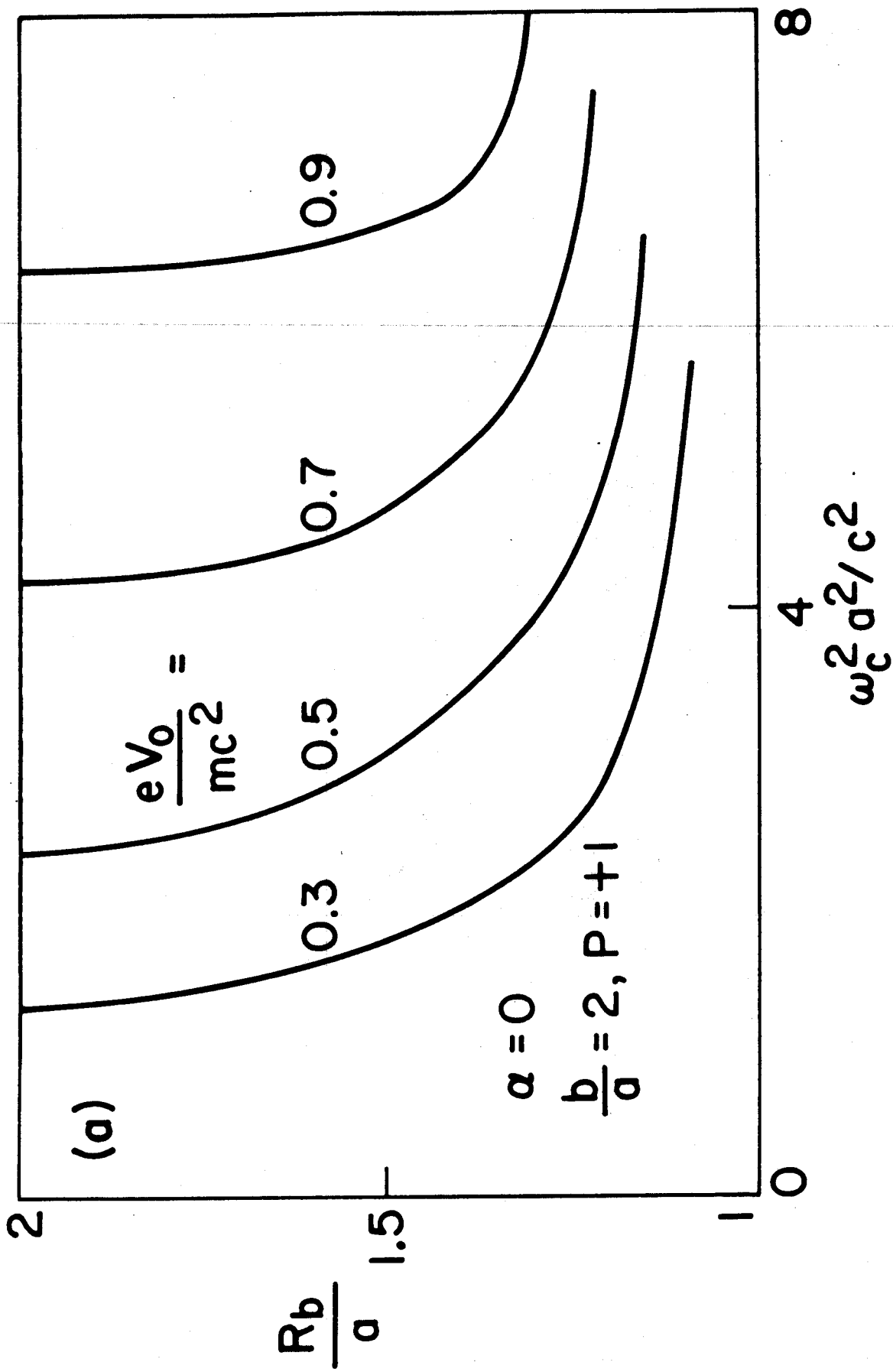


Fig. 5(a)

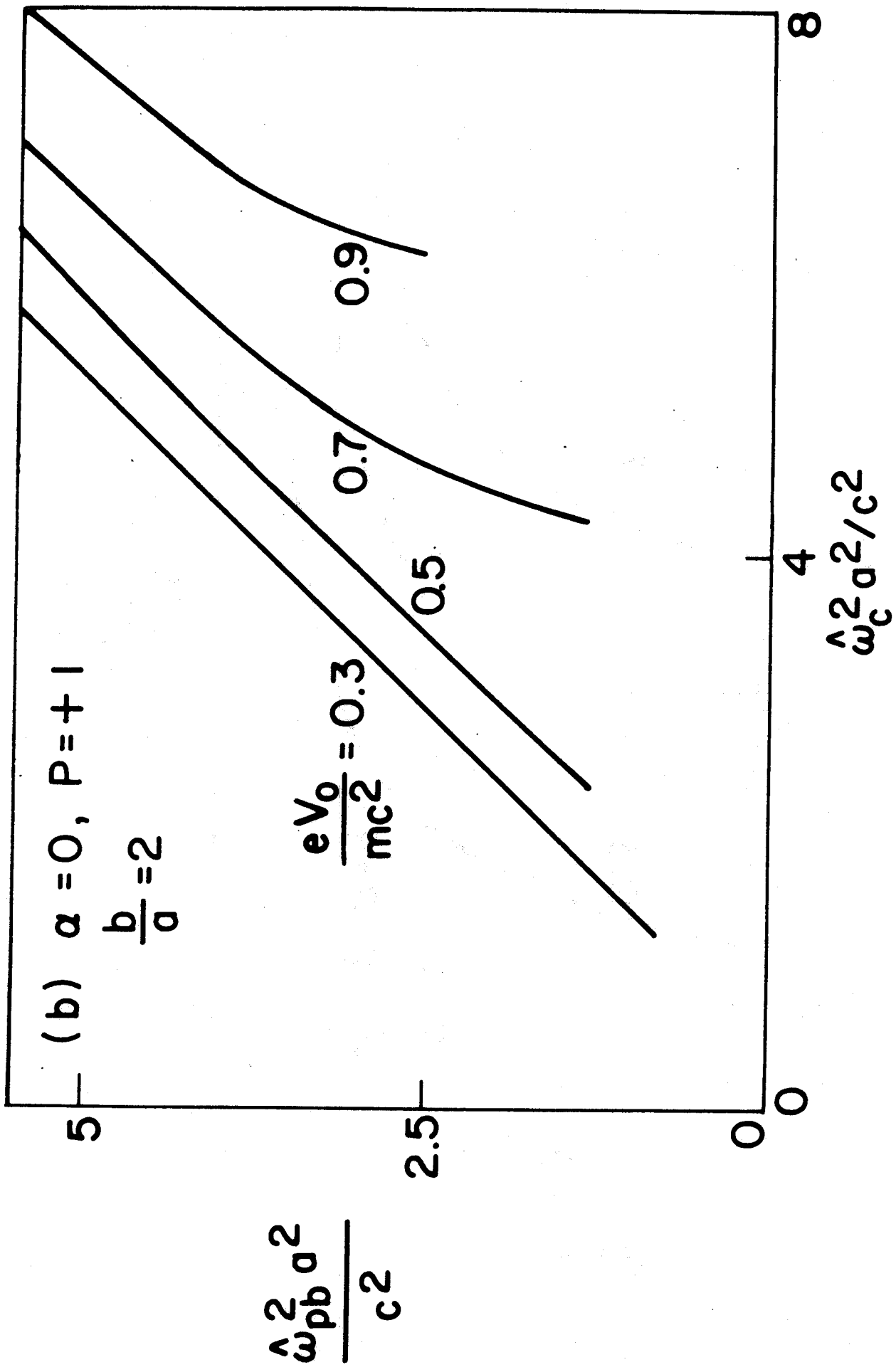


Fig. 5(b)

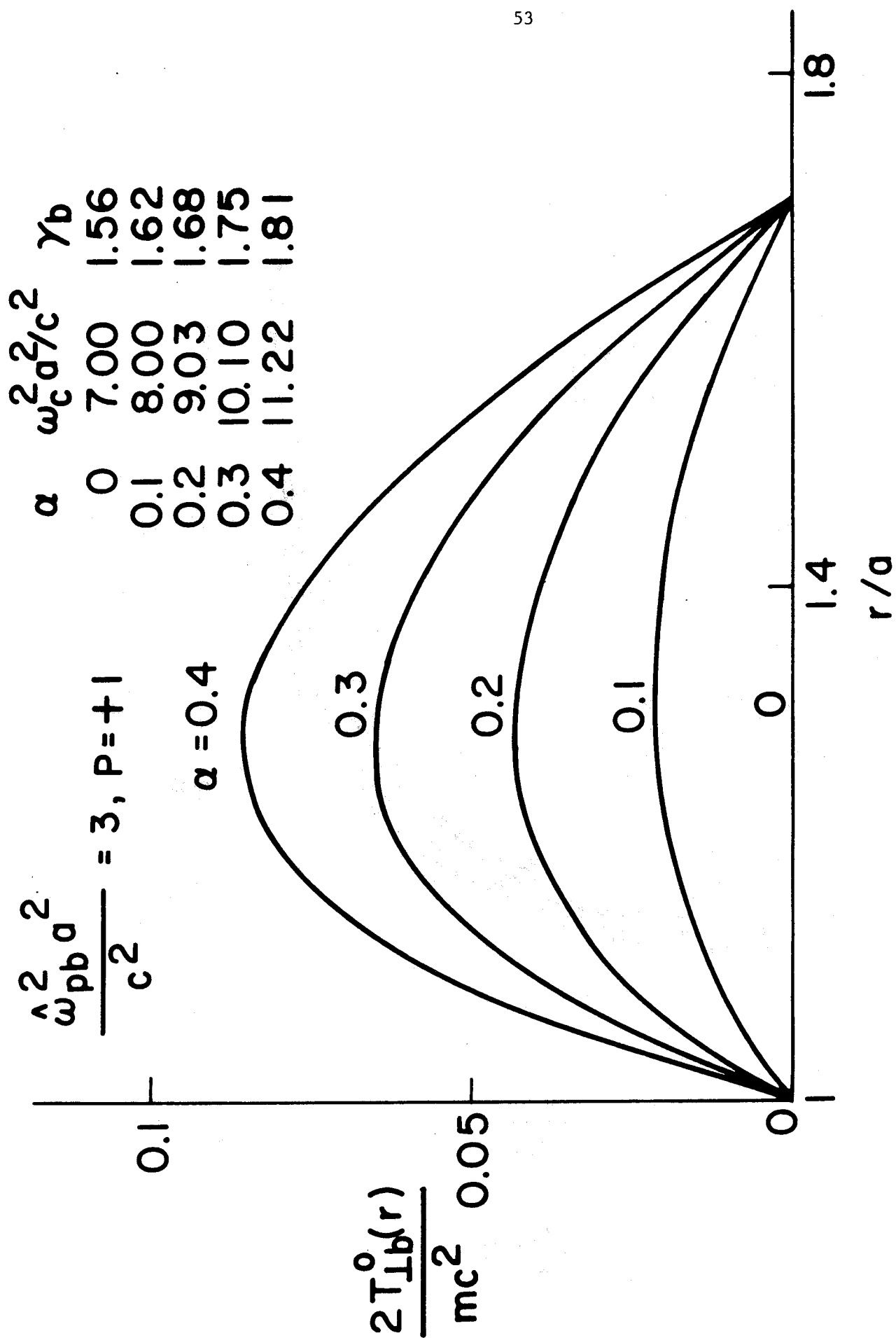


Fig. 6

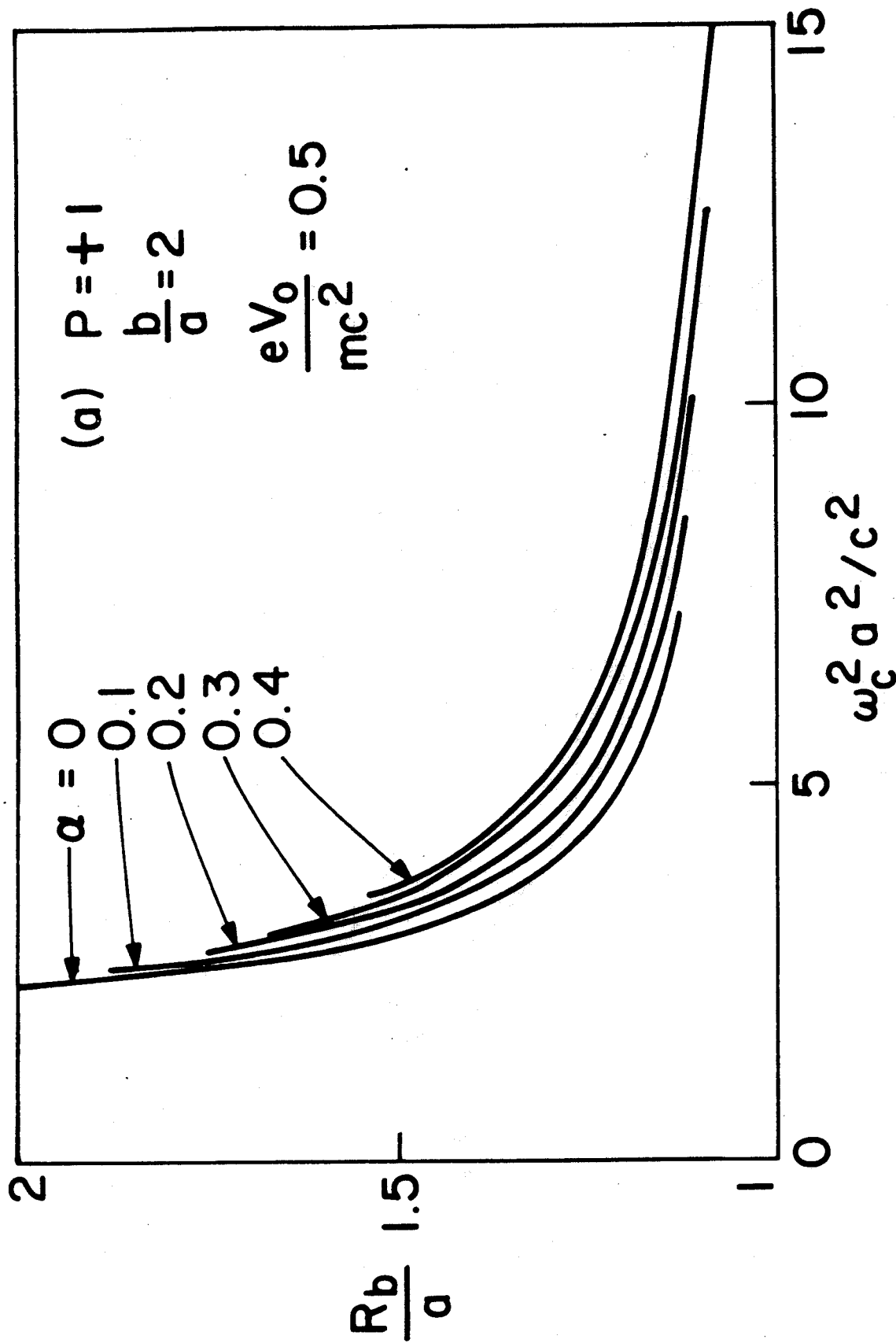


Fig. 7(a)

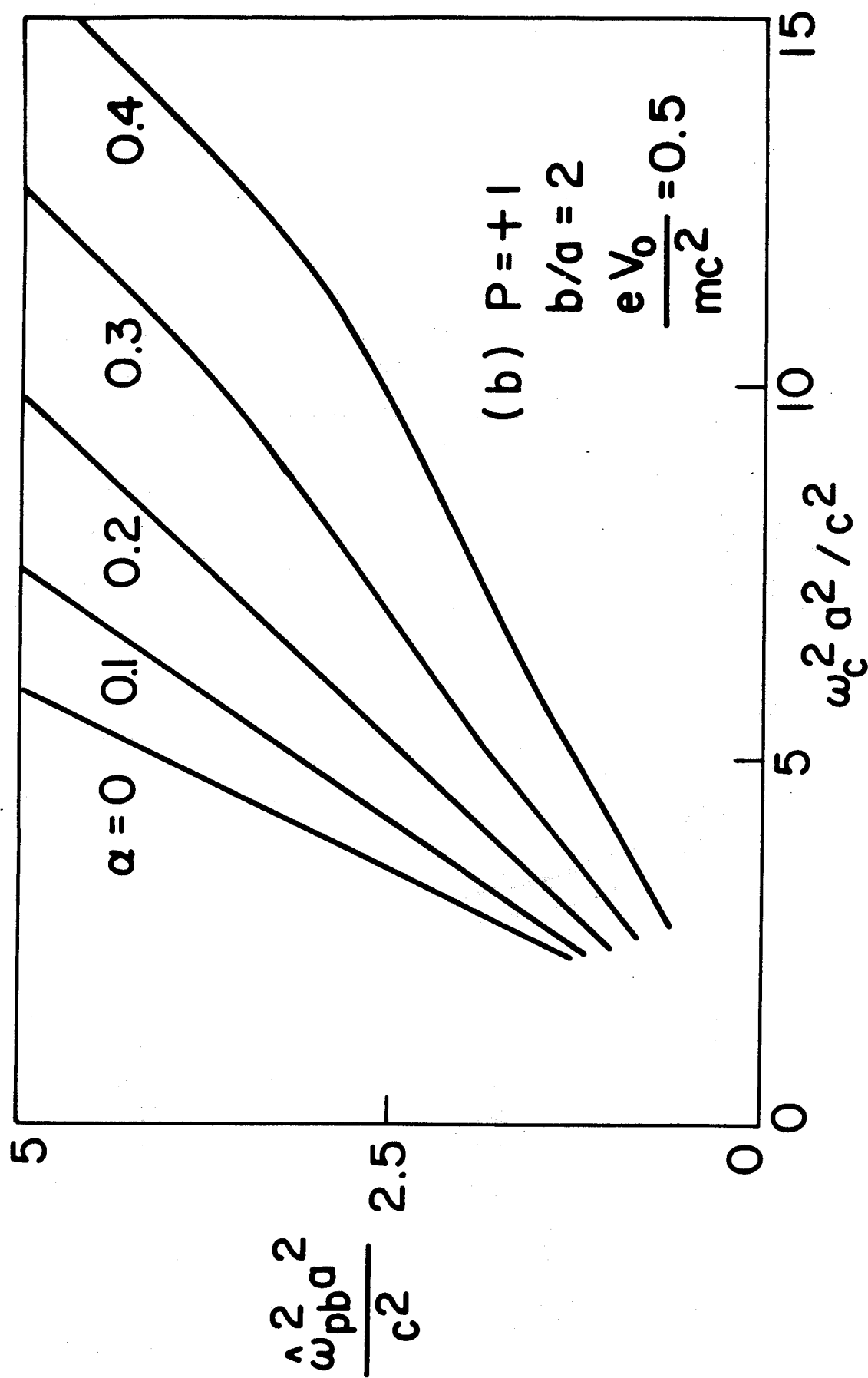


Fig. 7(b)

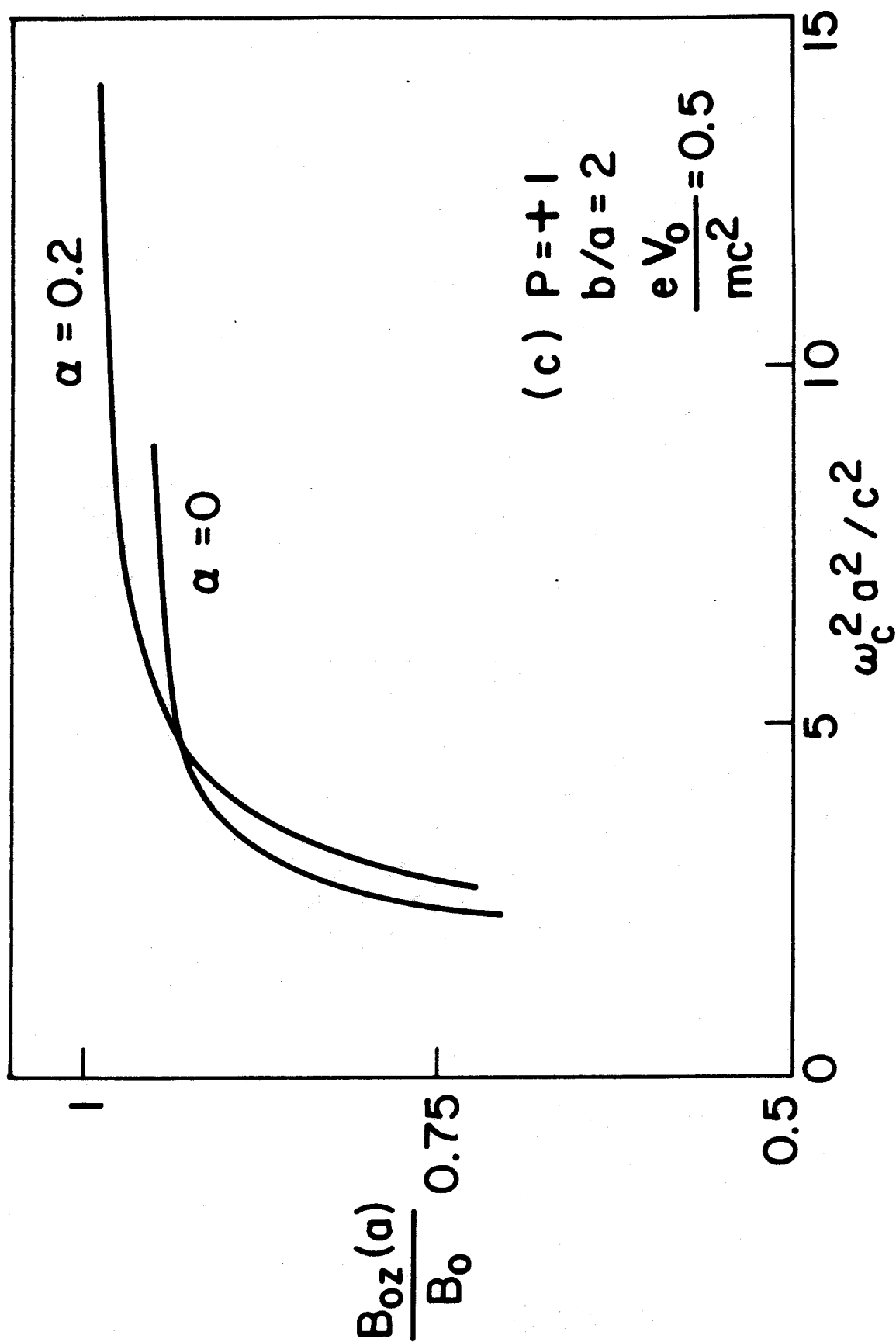


Fig. 7(c)

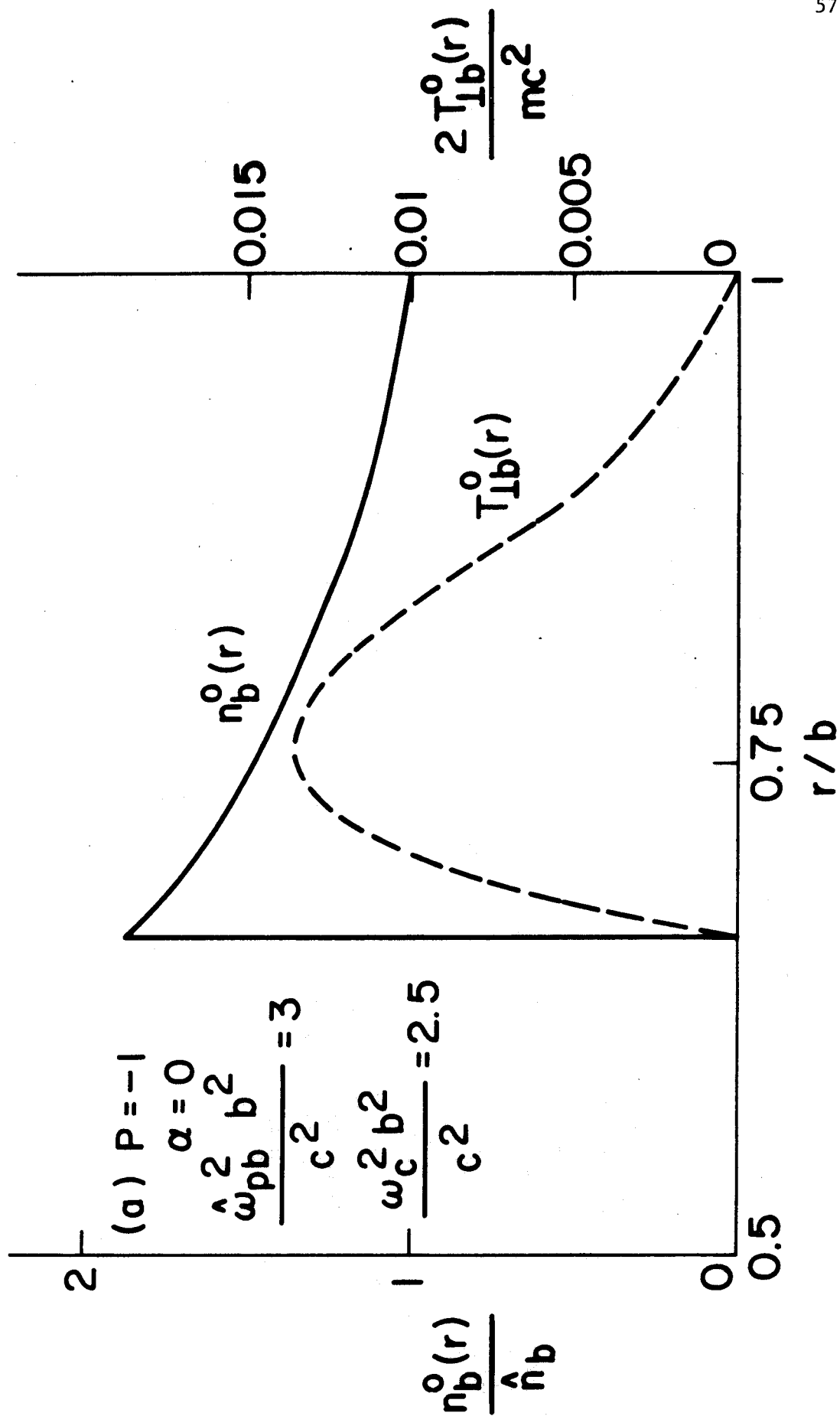


Fig. 8(a)

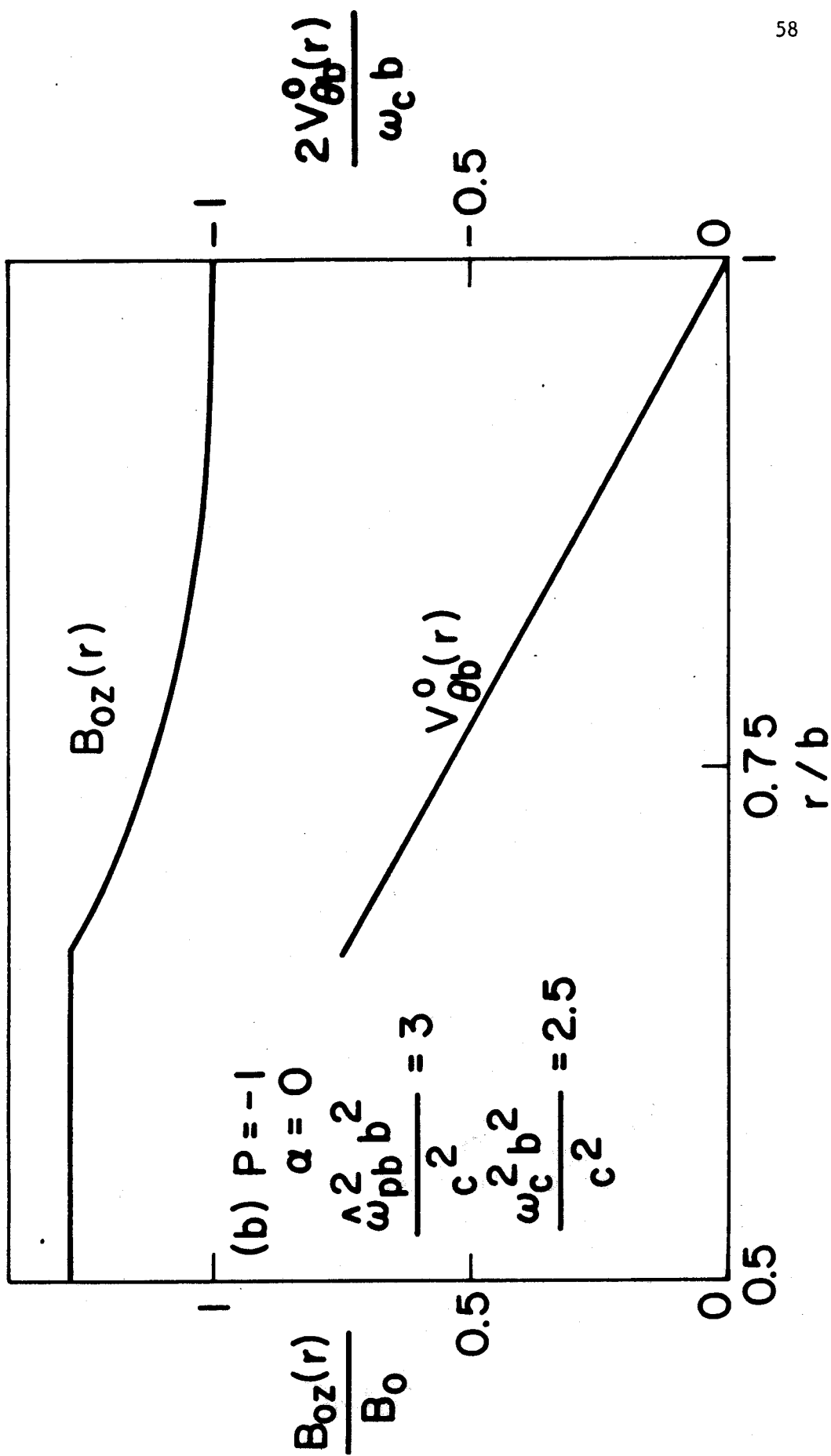


Fig. 8(b)

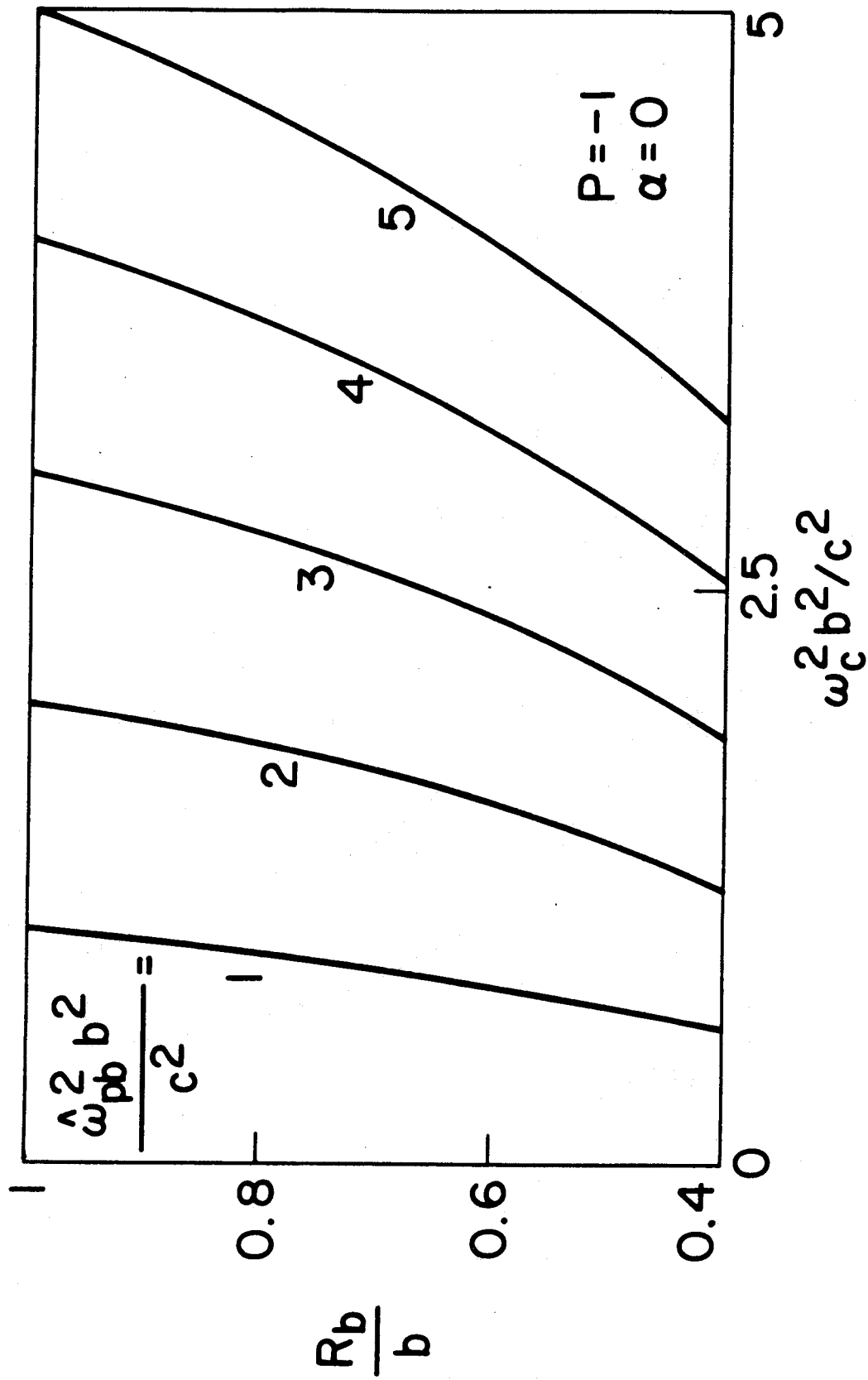


Fig. 9

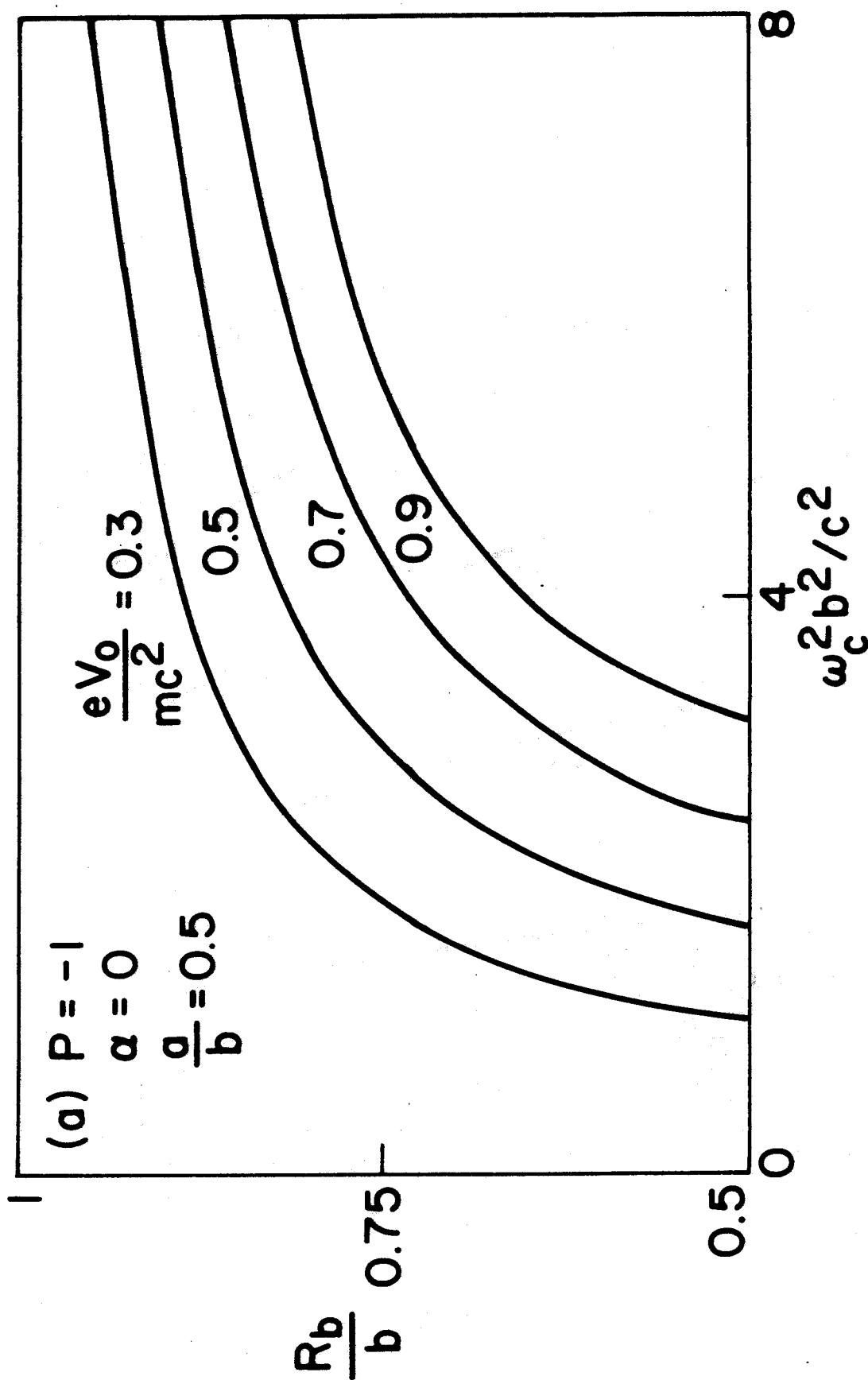


Fig. 10(a)

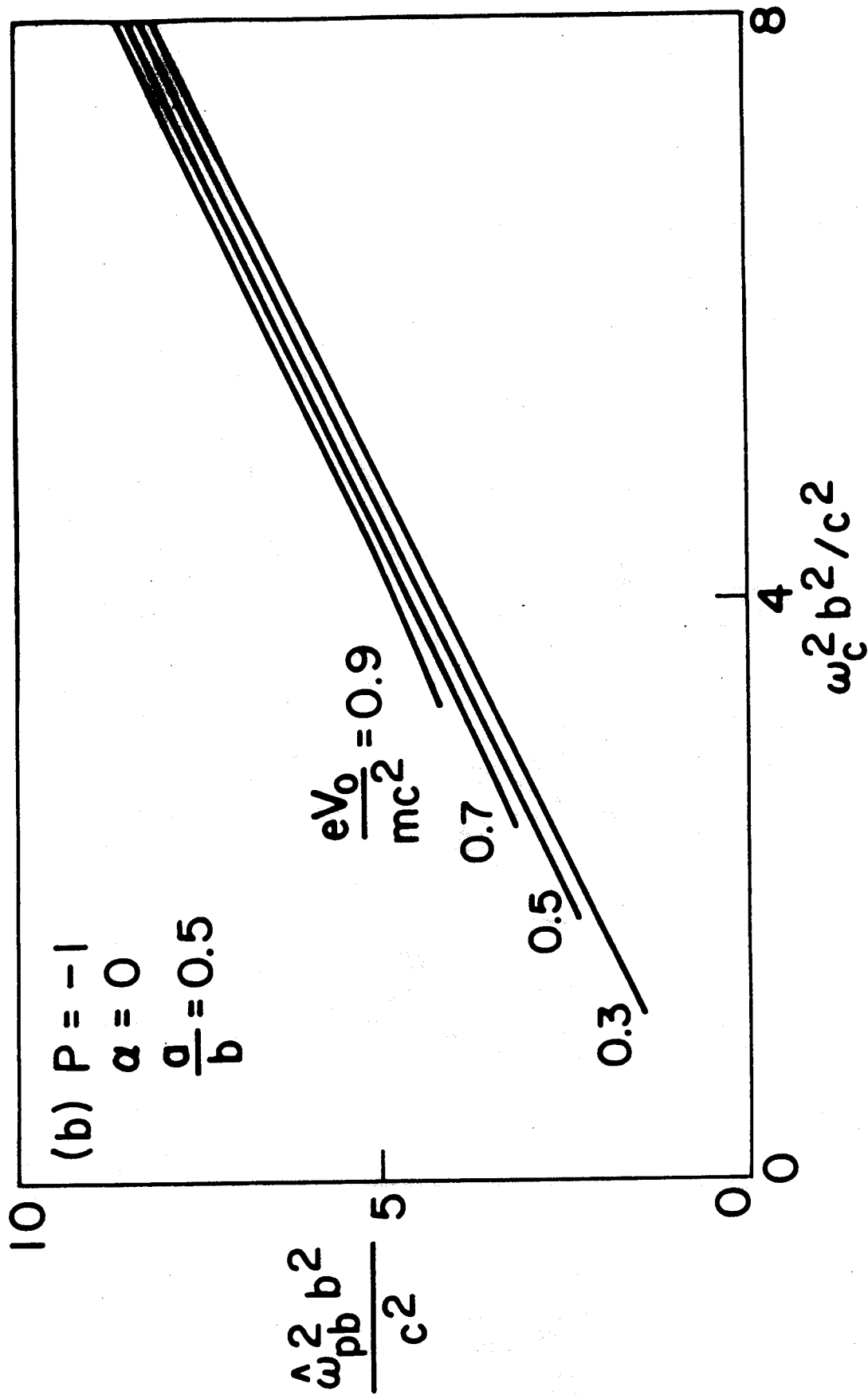


Fig. 10(b)

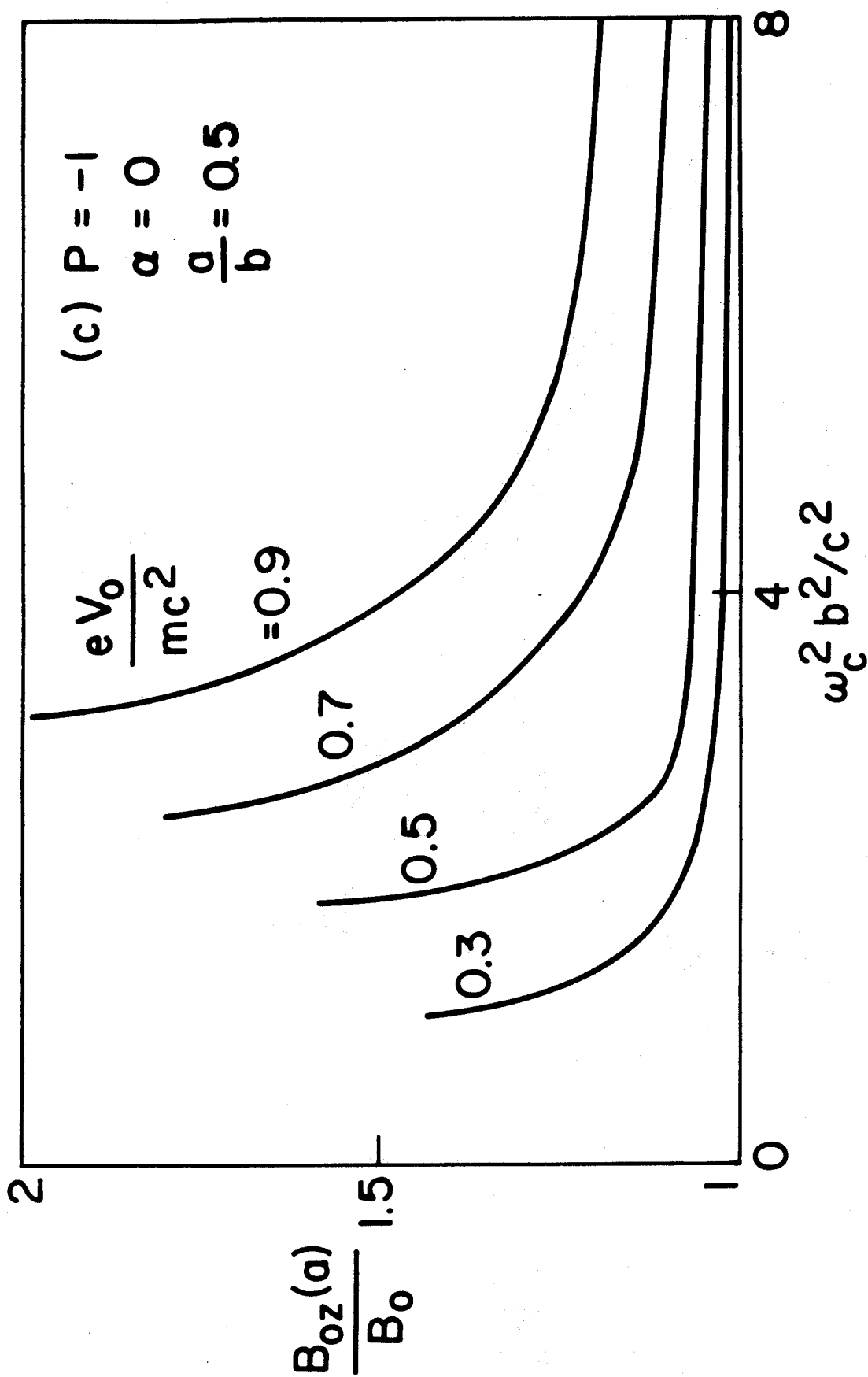


Fig. 10(c)

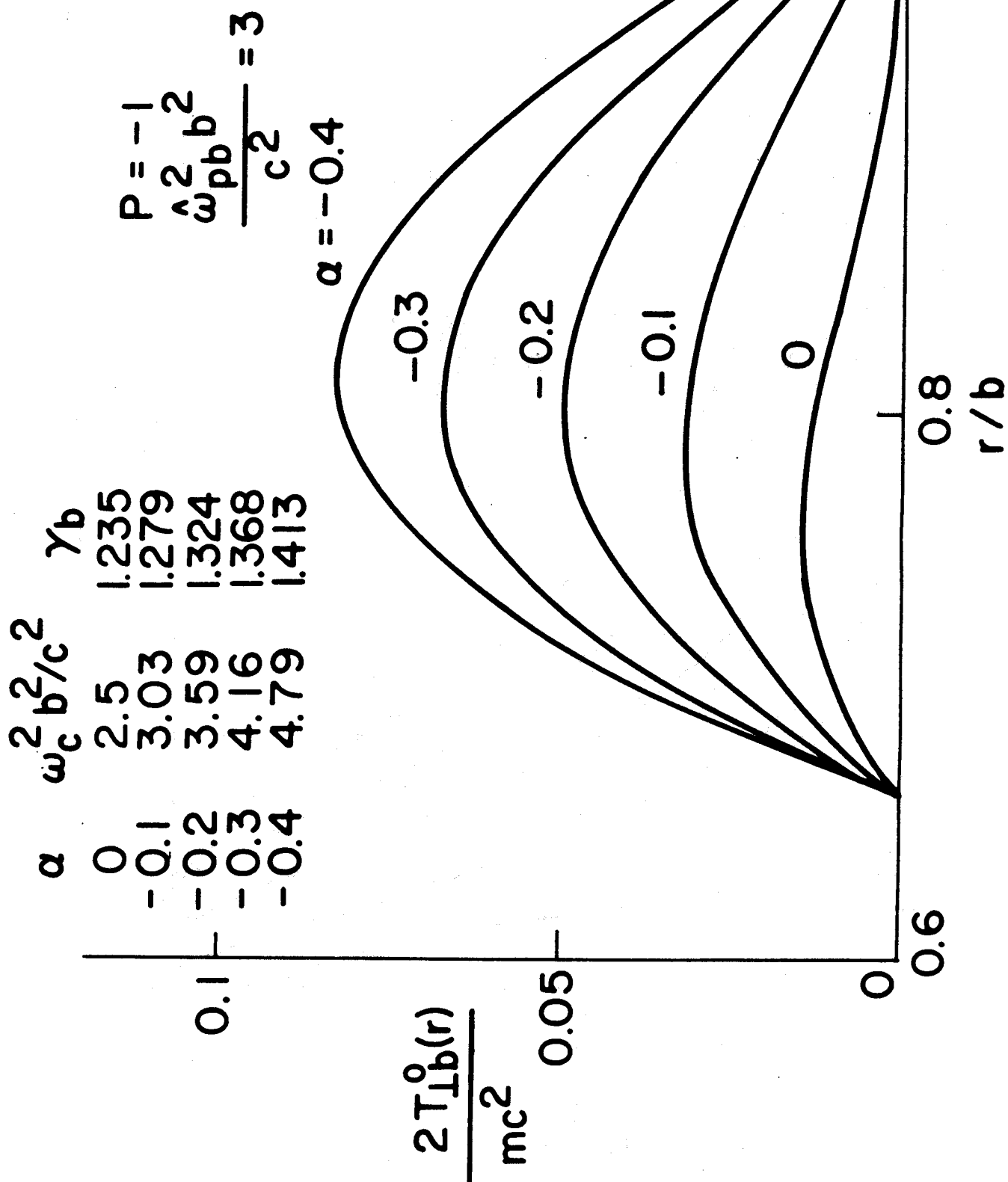


Fig. 11

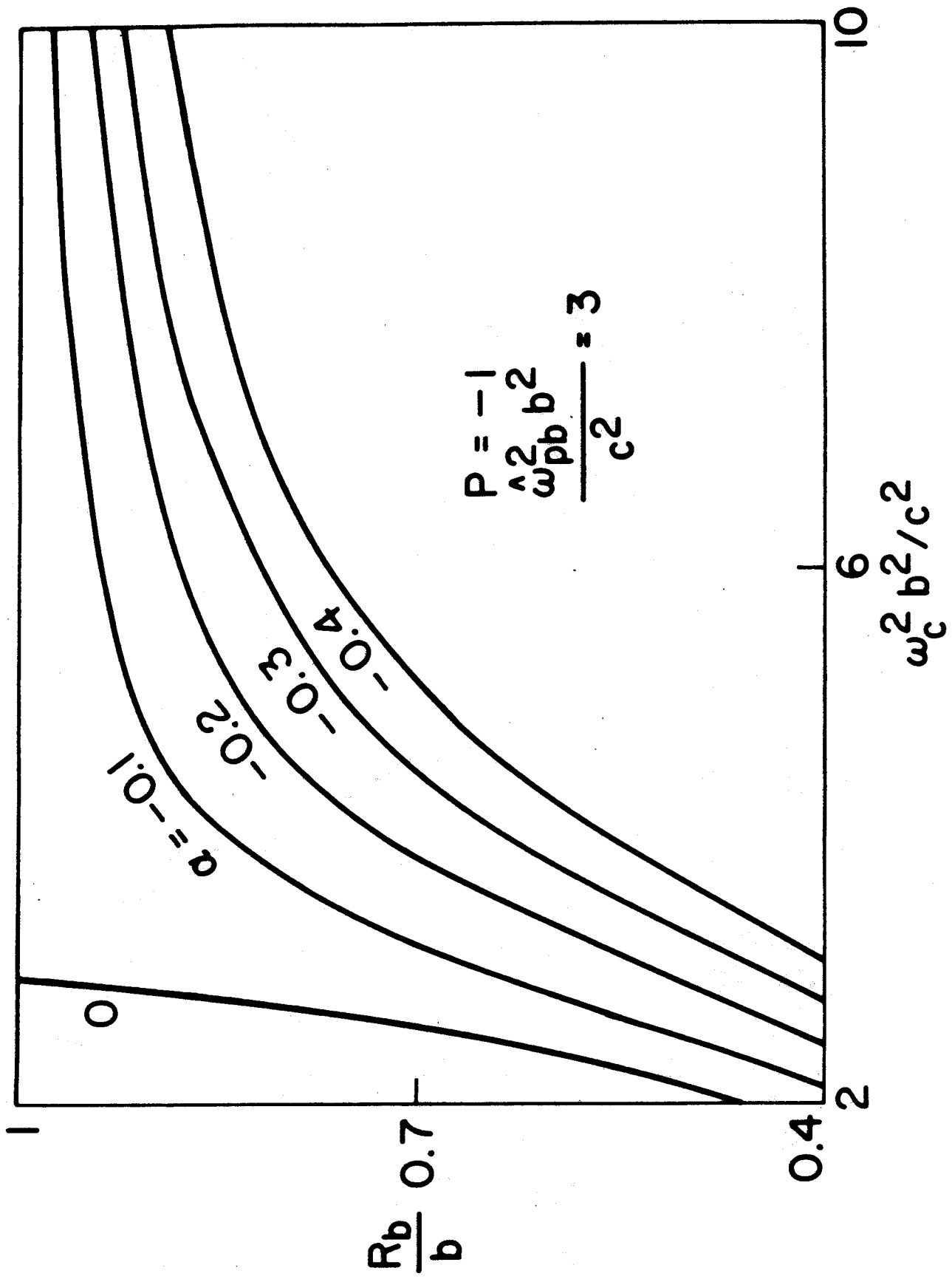


Fig. 12

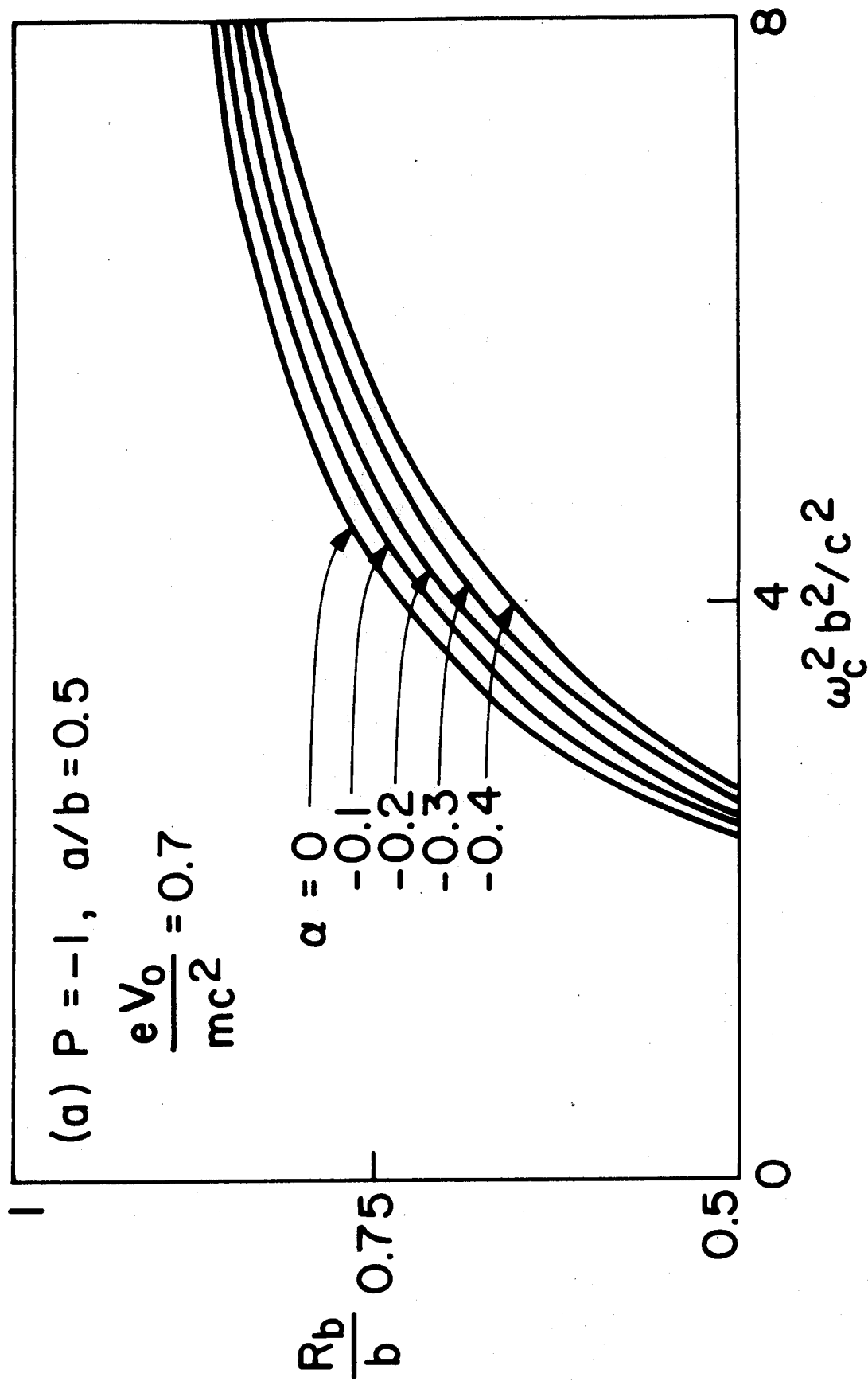


Fig. 13(a)

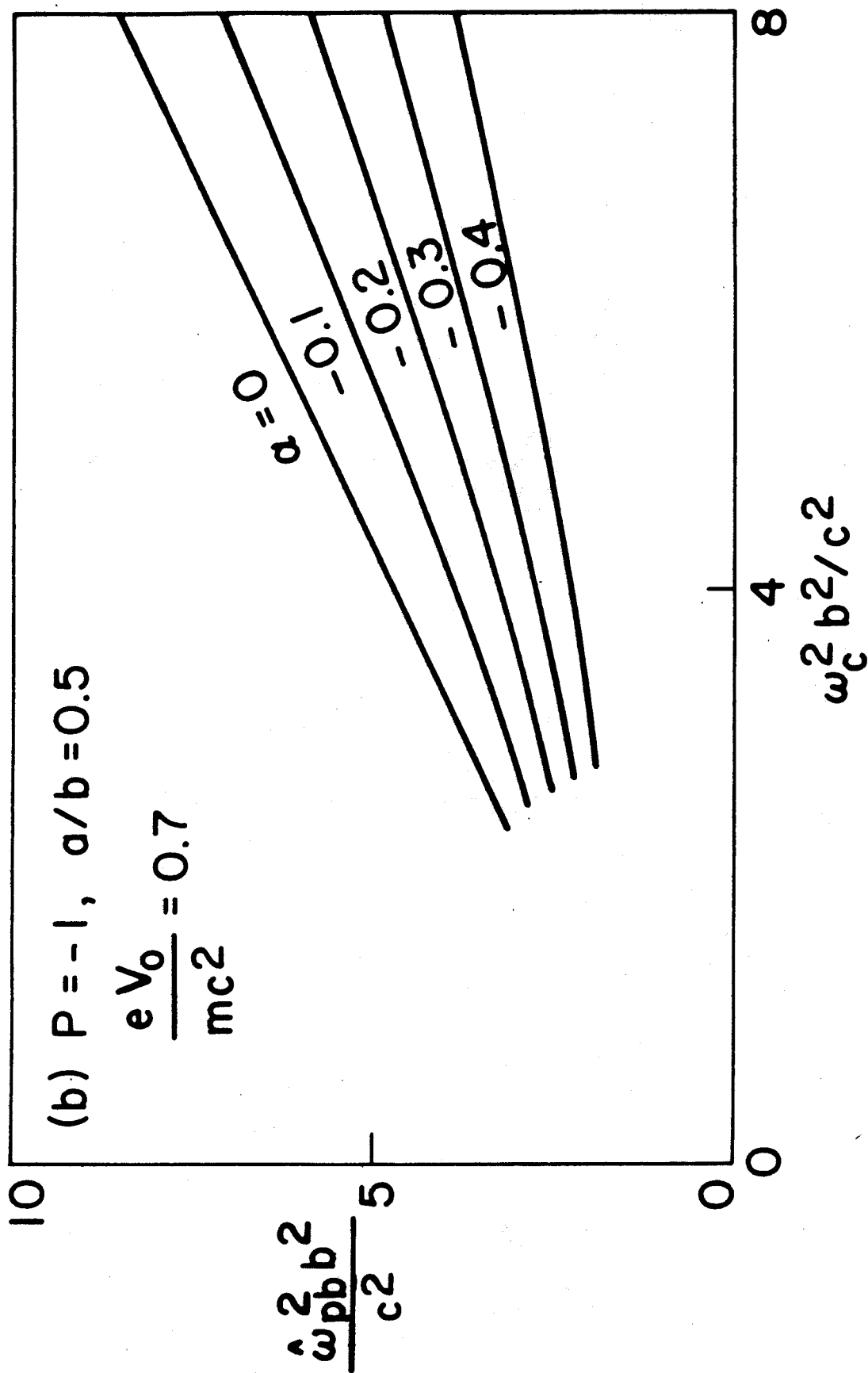


Fig. 13(b)